LIBRARY
[redacted]
NAVAL POSTGRADUATE SCHOOL
MONTEREY, CALIFORNIA 93940

NPS- 59PC7081A

UNITED STATES
NAVAL POSTGRADUATE SCHOOL

AD660006

HEAT TRANSFER AND FLOW FRICTION CHARACTERISTICS OF SEVERAL PLATE-FIN TYPE COMPACT HEAT EXCHANGER SURFACES

by

P. F. Pucci
S. F. Ball, Jr.
R. E. Traister

31 August 1967

This document has been approved for public release and sale; its distribution is unlimited.

FEDDOCS
D 208.14/2
NPS-59PC7081A

Feidon
L 202 4/2
NPS-53Fr 7081A

DUDLEY KNOX LIBRARY
NAVAL POSTGRADUATE SCHOOL
MONTEREY CA 93943-5101

NAVAL POSTGRADUATE SCHOOL
Monterey, California

Captain T. A. Melusky, USN
Acting Superintendent

Dr. R. F. Rinehart
Academic Dean

ABSTRACT:

Experimental results for the convective heat transfer and flow friction characteristics of plate-fin type heat transfer surfaces are presented for five surfaces. Four surfaces had a sinusoidal fin geometry. Two of these were fabricated of stainless steel, two of nickel. One of the nickel surfaces had perforated nickel fins. The fifth surface was fabricated of stainless steel and had a triangular fin geometry. The heat transfer data were obtained by the single-blow transient testing technique and by the cyclic testing technique. The two techniques compliment each other in extending the range of testing capability.

Table of Contents

	Page
Nomenclature	6
Introduction	9
Description of Surfaces	9
Experimental Method	10
Presentation of Results	12
Conclusions	12
References	13
Figures	14
Tables	33
Appendix A. Cyclic Testing Technique	39
Appendix B. Data Reduction Relationships	43
Appendix C. Description of Equipment	53
Appendix D. Perforated Nickel Geometric Properties	60

K LIBR
RADU
A 93943-

FIGURES PAGE

1. Schematic Diagram of Test Apparatus 14

2. Test Apparatus with Cyclic Power System 15

3. Heater and Test Section 16

4. Test Section with Matrix Removed 16

5. Nichrome Wire Heater 17

6. Geometric and Physical Properties of Solar No. 1 Matrix 18

7. Heat Transfer and Flow Friction Characteristics of Solar No. 1 Matrix 19

8. Geometric and Physical Properties of Solar No. 2 Matrix 20

9. Heat Transfer and Flow Friction Characteristics of Solar No. 2 Matrix 21

10. Geometric and Physical Properties of Solar No. 3 Matrix 22

11. Heat Transfer and Flow Friction Characteristics of Solar No. 3 Matrix 23

12. Geometric and Physical Properties of Solar No. 4 Matrix 24

13. Heat Transfer and Flow Friction Characteristics of Solar No. 4 Matrix 25

14. Geometric and Physical Properties of Solar No. 5 Matrix 26

15. Heat Transfer and Flow Friction Characteristics of Solar No. 5 Matrix 27

16. Comparison of Characteristics 28

17. Flow Area Goodness Factors for Solar No. 1 and 2 Matrices 29

18. Flow Area Goodness Factors for Solar No. 3, 4, and 5 Matrices 29

19. Heat Transfer Power versus Flow Friction Power for the Solar No. 1 and 2 Matrices 30

20. Heat Transfer Power versus Flow Friction Power for the Solar No. 3, 4 and 5 Matrices 30

21. NTU versus Amplitude Ratio 31

22. Perforated Nickel Geometry 32

23. Conduction Parameter Analog 32

TABLES | Page

I Summary Description of Matrices 33

II Summary of Friction and Heat Transfer Results 34

III Summary of Friction and Heat Transfer Results Solar No. 2 Matrix 35

IV Summary of Friction and Heat Transfer Results Solar No. 3 Matrix 36

V Summary of Friction and Heat Transfer Results Solar No. 4 Matrix 37

VI Summary of Friction and Heat Transfer Results Solar No. 5 Matrix 38

NOMENCLATURE

English Letter Symbols

A	Matrix total heat transfer area	sq ft
A_c	Matrix minimum free flow area	sq ft
A_{fr}	Matrix total frontal area	sq ft
A_s	Matrix solid cross sectional area available for thermal conduction	sq ft
A_k	Matrix solid cross sectional conduction area considering effect of matrix material perforations	sq ft
a_s	Fin thickness	ft
C_c	Jet contraction-area ratio for circular tube	dimensionless
c_p	Specific heat (gas) at constant pressure	Btu/(lbm deg F)
c_s	Matrix material specific heat	Btu/(lbm deg F)
C_f	Flow stream capacity rate ($\dot{m}c_p$)	Btu/(hr deg F)
C_s	Matrix heat capacity ($W_s c_s$)	Btu/(deg F)
D_H	Hydraulic diameter of internal passage	ft
E	Friction power expended per unit of surface heat transfer area	hp/sq ft
G	Matrix flow stream mass velocity ($\dot{m}/Ac$)	lbm/(hr sq ft)
g_c	Proportionality factor in Newton's Second Law	32.2 (lbm ft)/(lbf sec^2)
h	Thermal convection surface heat transfer coefficient; heat transfer power per unit area per degree temperature difference	Btu/(hr sq ft deg F)
K_c	Loss coefficient for sudden flow contraction at matrix entrance	dimensionless

K_d	Momentum velocity-distribution coefficient	dimensionless
K_e	Loss coefficient for sidden flow expansion at matrix exit	dimensionless
k	Unit thermal conductivity	Btu/(hr sq ft deg F/ft)
k_s	Matrix material thermal conductivity	Btu/(hr sq ft deg F/ft)
k_y	Thermal conductivity in radial direction	Btu/(hr sq ft deg F/ft)
L	Total matrix flow length	ft
$\dot{m}$	Mass flow rate	lbm/hr
P	Pressure	lbf/sq ft
P	Matrix porosity (A_c/A_{fr})	dimensionless
q	Heat transfer rate	Btu/hr
R	Universal gas constant (53.35 for air)	(ft lbf)/(lbm deg R)
r_H	Hydraulic radius (A_cL/A_b)	ft
S^*	Relative shape factor	dimensionless
t	Temperature	deg F
u	Flow velocity	ft/sec
V_m	Matrix volume	cu ft
V_s	Matrix material volume (corrected for effects of perforations)	cu ft
W_s	Matrix mass	lbm
x	Distance from matrix inlet in flow direction	ft

Subscripts

atm	Local atmosphere
ave	Average
f	Fluid (gas, air)
i	Initial, inlet, individual

m	Mean, matrix
o	At orifice
s	Solid (matrix material), static
STD	Standard (temperature and pressure)
x	Local conditions
1	At inlet (upstream of heating elements)
2	At matrix inlet (downstream of heating)
3	At matrix exit

Greek Letter Symbols

β	Area density: compactness (ratio of matrix total heat transfer area to core volume-A/V)	sq ft/cu ft
$\bar{\beta}$	Diameter ratio, do/d	dimensionless
Δ	Difference or change (time, distance, temperature)	
Θ	Time	Sec, hr.
μ	Fluid viscosity (dynamic)	lbm/hr ft
ν	Specific volume	ft^3/lbm
ρ	Density	lbm/cu ft
σ	Ratio of free flow to frontal area (A_c/A_{fr})	dimensionless
ω_o	Angular frequency of temperature oscillation	rad/sec

Dimensionless Groupings

α	Amplitude attenuation parameter
f	Fanning friction factor (Ratio of wall shear stress to the fluid dynamic head). This factor is plotted versus N_R to illustrate the flow friction characteristics of a matrix surface.

j	Colburn Factor ($N_{st}N_{pr}$), a generalized heat transfer grouping. This factor is plotted versus N_R to illustrate heat transfer characteristics of a matrix surface.
M	Flow parameter ($\dot{m}c_p/Wc_s\ \omega_o$)
N_{Nu}	Nusselt number (hD_h/k), a heat transfer modulus
N_{Pr}	Prandtl number ($\mu c_p/k$), a fluid properties modulus
N_R	Reynolds number (D_hG/μ), a flow modulus
N_{St}	Stanton number (h/Gc_p), a heat transfer modulus
Ntu	Number of heat transfer units ($hA/\dot{m}c_p$), a heat transfer parameter
R	Ratio of matrix outlet temperature amplitude to matrix inlet temperature amplitude during cyclic temperature variation
λ	Longitudinal heat conduction parameter for solid matrix material ($k_sA_s/\dot{m}Lc_p$).
ξ	Distance parameter (x/L)
τ	Time parameter ($hA/W_s\ C_s$) used in Single-Blow analysis (17)
$\bar{\tau}$	Time parameter ($\mu\Theta/L$) used in cyclic technique
ω	Frequency parameter (ω_oL/u) used in cyclic technique

INTRODUCTION

This document reports the results obtained during FY66 and FY67 of a continuing program for the evaluation of the heat transfer and fluid friction characteristics of compact heat exchanger surfaces at the Naval Postgraduate School, Monterey. Results obtained in FY65 have been previously reported [1], [2][1].

DESCRIPTION OF SURFACES

The five surfaces tested, manufactured and provided by Solar, a division of International Harvester, San Diego, had basically sinusoidal or triangular fins in a plate-fin geometry. Table I is a summary of the matrix geometries. Only one matrix tested, designated Solar #3, was brazed. All matrices had a frontal cross section of approximately 3 and 1/16 inches square and a length of approximately 3. inches in the flow direction. The perforated nickel plate fins of the Solar #2 matrix is an electro-deposited metallic sheet of integral structure manufactured by Perforated Products, Incorporated, and is described in Appendix D.

[1] Numbers in brackets refer to numbered items listed in References.

EXPERIMENTAL METHODS

To obtain the heat transfer data, two testing techniques were employed: the single-blow, transient testing technique and the cyclic testing technique.

The single-blow, transient testing technique is completely described in reference [2], however, briefly this method consists of heating the test matrix by heated air to a uniform temperature (approximately 20.F above ambient temperature in these tests) and then subjecting the matrix to a step change in the air flow temperature to ambient temperature. The air temperature downstream of the matrix is monitored and recorded versus time. The test rig used in these tests is shown in Figures 1-5, and described in detail in Appendix C. A series of fine nichrome wire heaters were installed upstream of the matrix to heat the air. Turning off the heaters provides the step change in the temperature of the air without disturbing the flow. By referencing the thermocouples downstream of the matrix to the thermocouples upstream of the heaters, the initial temperature difference can be very closely controlled. This temperature difference is continuously recorded by a strip chart recorder when a run is made. This recorded trace has the distinct advantage that there is no transposition of data required which would produce increased uncertainties. Reduction of the data follows the method of Locke [6] and Howard [4], whereby the Ntu of the surface can be evaluated by determining the maximum slope of the fluid temperature difference versus time curve during the cooling transient.

The cyclic testing technique is completely described in reference [5]. However, briefly this method consists of producing a sinusoidal time varying temperature of the steady air flow to the matrix. This air inlet temperature and the time varying temperature of the outlet air downstream of the matrix are monitored and simultaneously recorded. The test rig used was the same as that used for the above single-blow transient tests. A low frequency sinusoidal voltage was superimposed on an appropriate d.c. level and fed to the nichrome heaters. Reduction of the data follows the method of Bell and Katz [5], whereby the Ntu of the surface can be evaluated by determining the ratio of output to input amplitudes of the temperature variations. See Appendix A. Again, recording these temperatures directly and simultaneously, requiring no transposition of data, reduces the data reduction uncertainties.

PRESENTATION OF RESULTS

Heat transfer and flow friction data for each of the matrices tested are given in both tabular and graphical form, TABLES I through IV and Figures 6 through 15, using the Colburn-j modulus, Fanning friction factor, and Reynolds number.

Figure 16 is a summary plot comparing the heat transfer and flow friction characteristics of the matrices tested.

Figures 17 and 18 present "figure of merit" type curves. The j/f versus Reynolds number thus plotted gives an indication of the matrix flow frontal area required for a given pressure drop.

Figures 19 and 20 present curves of heat transfer power versus flow friction power on a unit area basis, evaluated for fluid properties at standard conditions of dry air at 500.F and one atmosphere.

CONCLUSIONS

Of the five matrices tested, the Solar No. 2 matrix with sinusoidal fin geometry of perforated nickel, exhibited the best overall performance particularly at the higher Reynolds Numbers tested.

The three stainless steel matrices, Solar Nos. 3, 4, and 5, exhibited essentially the same overall characteristics. The triangular fin geometry of Solar No. 5 exhibited a slightly higher friction factor with a resulting lower j/f than the sinusoidal fin geometries.

The employment of the cyclic testing technique appears to be an effective means for extending the range of testing for the facility originally designed for the single-blow transient testing technique.

REFERENCES

1. Bannon, J. M., Piersall, C. H. Jr., Pucci, P. F., "Heat Transfer and Flow Friction Characteristics of Perforated Nickel Plate-Fin Type Heat Transfer Surfaces." Technical Report No. 52, U. S. Naval Postgraduate School, Monterey, California, 1965.

2. Pucci, P. F., Howard, C. P., and Piersall, C. H. Jr., "The Single-Blow Transient Testing Technique for Compact Heat Exchanger Surfaces", Trans. ASME, Journal of Engineering for Power, Vol. 89, Ser. A, No. 1 Jan. 1967, pp. 29-40.

3. Ball, Stuart F., "Experimental Determination of Heat Transfer and Flow Friction Characteristics for Several Plate Fin Type Compact Heat Exchanger Surfaces." Master's Degree Thesis, U. S. Naval Postgraduate School, Monterey, California, 1966.

4. Howard, C. P., "The Single Blow Problem Including the Effects of Longitudinal Conduction", ASME paper number 64-GTP-11, 1964.

5. Bell, J. C. and Katz, E. F., "A Method for Measuring Surface Heat Transfer Using Cyclic Temperature Variations." *Heat Transfer and Fluid Mechanics Institute*, Berkeley, California, 1949.

6. Locke, G. L. "Heat Transfer and Flow Friction Characteristics of Porous Solids", TR. No. 10, Department of Mechanical Engineering, Stanford University, Stanford, California, 1 June 1950.

7. American Society of Mechanical Engineers. *Power Test Code Supplements, Instruments and Apparatus*, PTC-19.5;4, Flow Measurements, Chapt. 4, New York: ASME 1959.

8. Murdock, J. W., "Tables for Interpolation and Extrapolation of ASME Coefficients for Square-Edged Concentric Orifices", ASME, paper No. 64-WA/FM-6.

9. Kays, W. M., "Loss Coefficients for Abrupt Changes in Flow Cross Section with Low Reynolds Number Flow in Single and Multiple-Tube Systems, *Transactions, ASME*, Vol. 72, pp 1067-1074, 1950.

10. Kays, W. M. and London, A. L., *Compact Heat Exchangers*. Second Edition, New York: McGraw-Hill Book Company, Inc., 1964.

11. Dayton, R. W., et. al. "Improved Measurements of Surface Heat Transfer by the Methods of Cyclic Temperature Variations," BMI-747, Battelle Memorial Institute, 28 May 1952.

12. Chastain, J. W. and Dinger, D.A., "A Study of Error Effects in Measuring Cyclic-Temperature Heat-Transfer Coefficients." Rpt. No. BMI-1167, ENGINEERING (TID-4500, 12th Ed.), Battelle Memorial Institute, Columbus, Ohio, 15 February 1957.

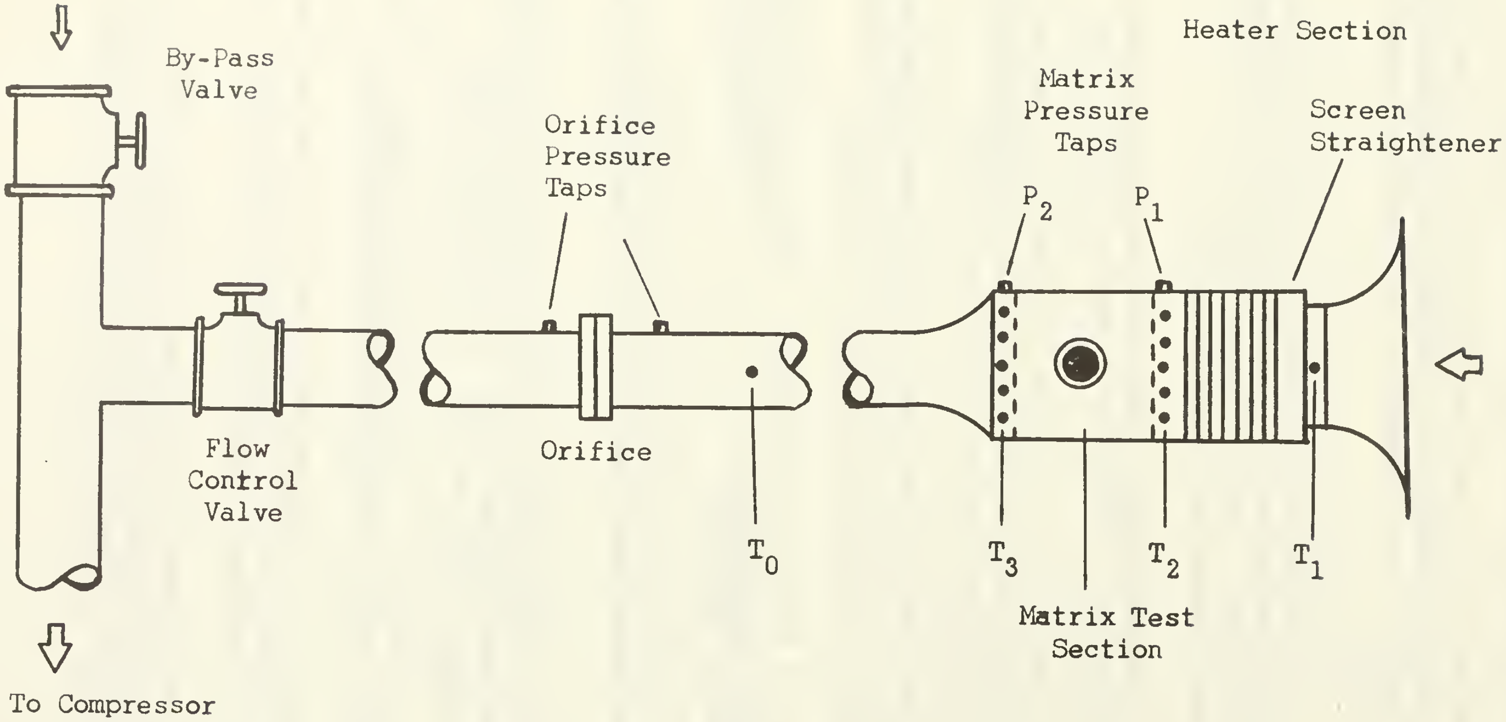

Figure 1. Schematic Diagram of Test Apparatus.

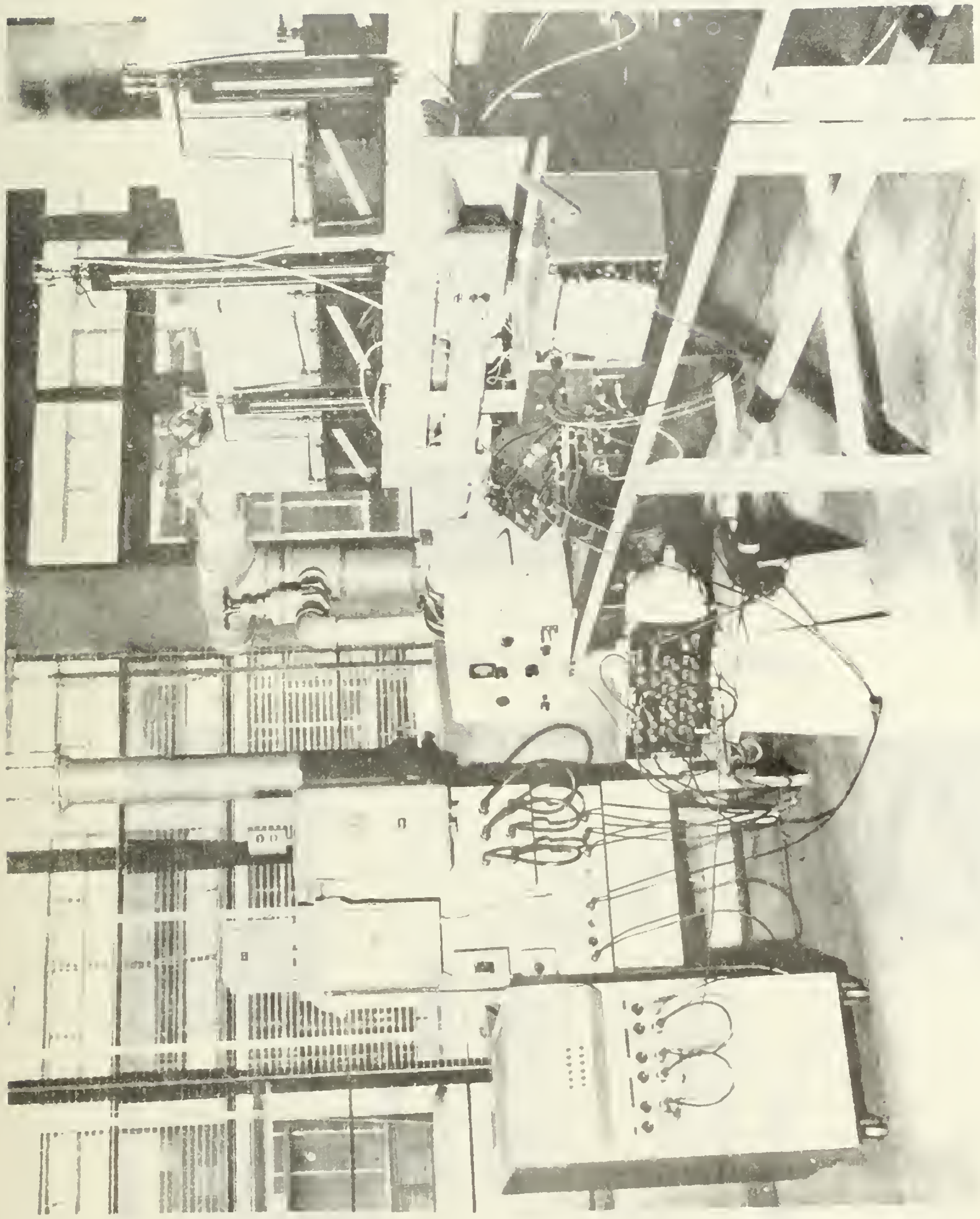

Figure 2. Test Apparatus with Cyclic Power System.

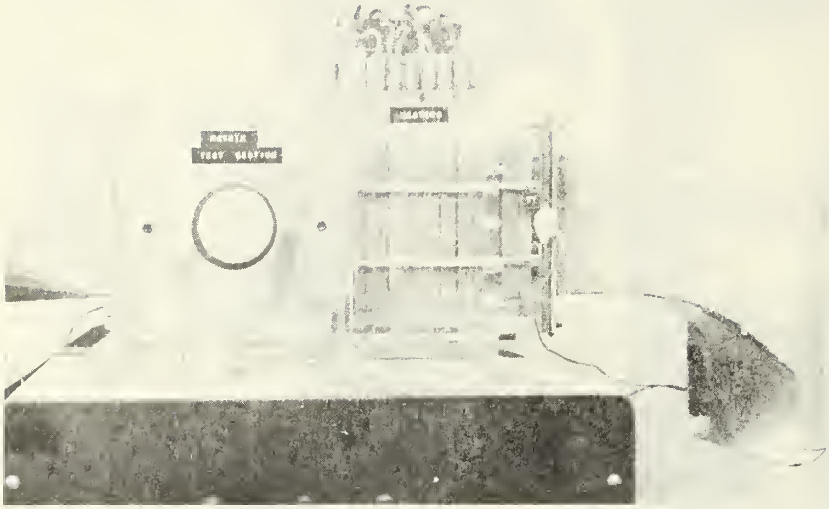

Figure 3. Heater and Test Section.

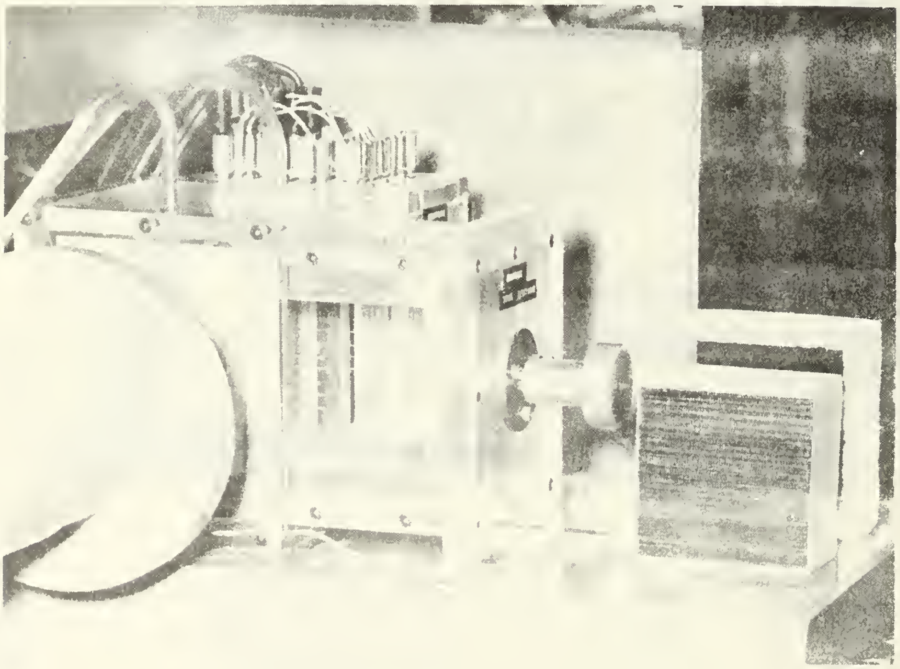

Figure 4. Test Section with Matrix Removed.

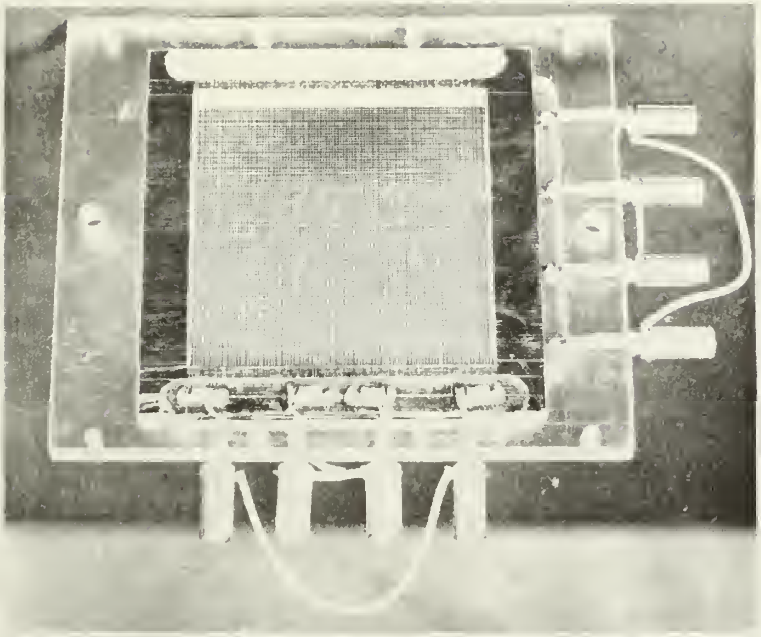

Figure 5. Nichrome Wire Heater.

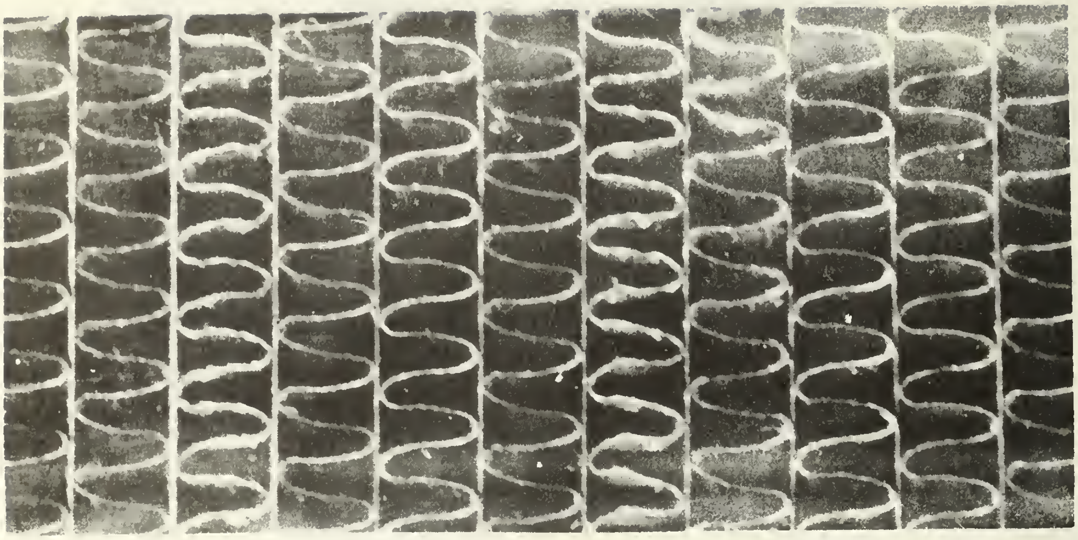

SOLAR # 1

Matrix Material		Nickel
Specific Heat, c_s	(Btu/lbm deg F)	.106
Thermal Conductivity, k_s	(Btu/hr fr deg F)	38.7
Material Thickness, a_s	(in)	.005
Total Heat Transfer Area, A	(sq ft)	12.768
Frontal Area, A_{fr}	(sq ft)	.07022
Conduction Area, A_s	(sq ft)	.01078
Free Flow Area, A_c	(sq ft)	.05944
Matrix Flow Length, L_m	(ft)	.24917
Matrix Volume, V_m	(cu ft)	.0175
Matrix Density, ρ_m	(lbm/cu ft)	86.1378
Compactness, β	(sq ft/cu ft)	729.7026
Porosity, p		.8464
Hydraulic Diameter, D_h	(ft)	.0046395

Figure 6. Geometric and Physical Properties of Solar #1 Matrix

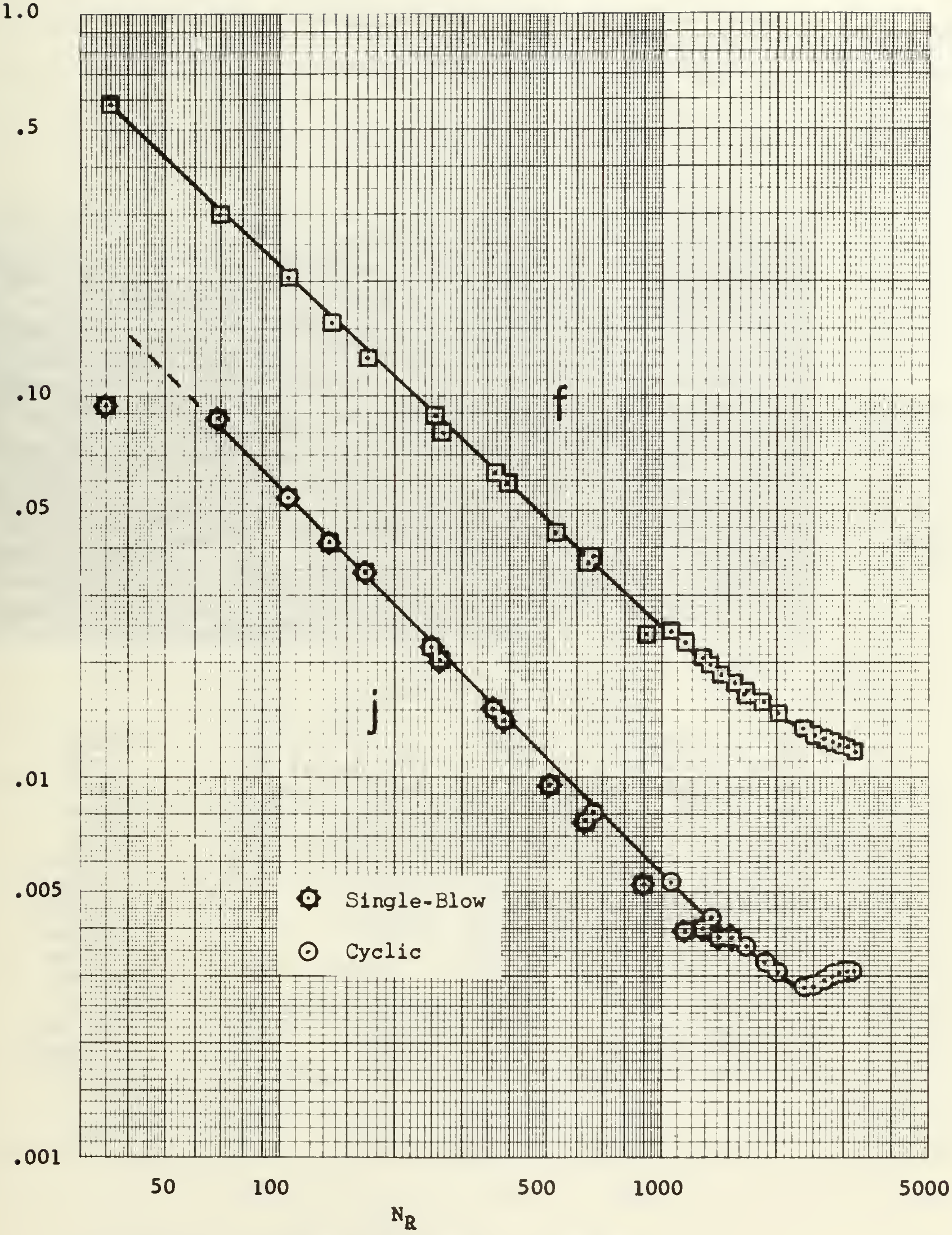

Figure 7. Heat Transfer and Flow Friction Characteristics of Solar No. 1 Matrix.

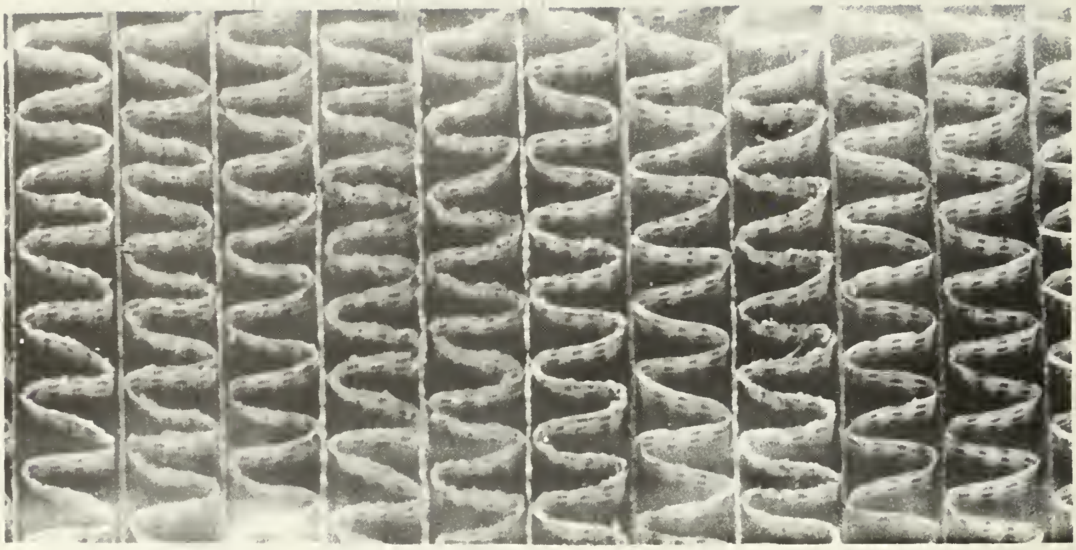

SOLAR # 2

Matrix Material		**Nickel**
Specific Heat, c	(Btu/lbm deg F)	.106
Thermal Conductivity, k_s	(Btu/hr ft deg F)	38.7
Splitter Thickness, a_s	(in)	.005
Total Heat Transfer Area, A	(sq ft)	12.093
Frontal Area, A_{fr}	(sq ft)	.07022
Conduction Area, A_s	(sq ft)	.01034
Free Flow Area, A_c	(sq ft)	.05987
Matrix Flow Length, L_m	(ft)	.25583
Matrix Volume, V_m	(cu ft)	.01797
Matrix Density, ρ_m	(lbm/cu ft)	70.3099
Compactness, β	(sq ft/cu ft)	673.143
Porosity, p		.85281
Hydraulic Diameter, D_h	(ft)	.0046272
Perforated Fin Material	.0047" thick	80/20T

Figure 8. Geometric and Physical Properties of Solar #2 Matrix

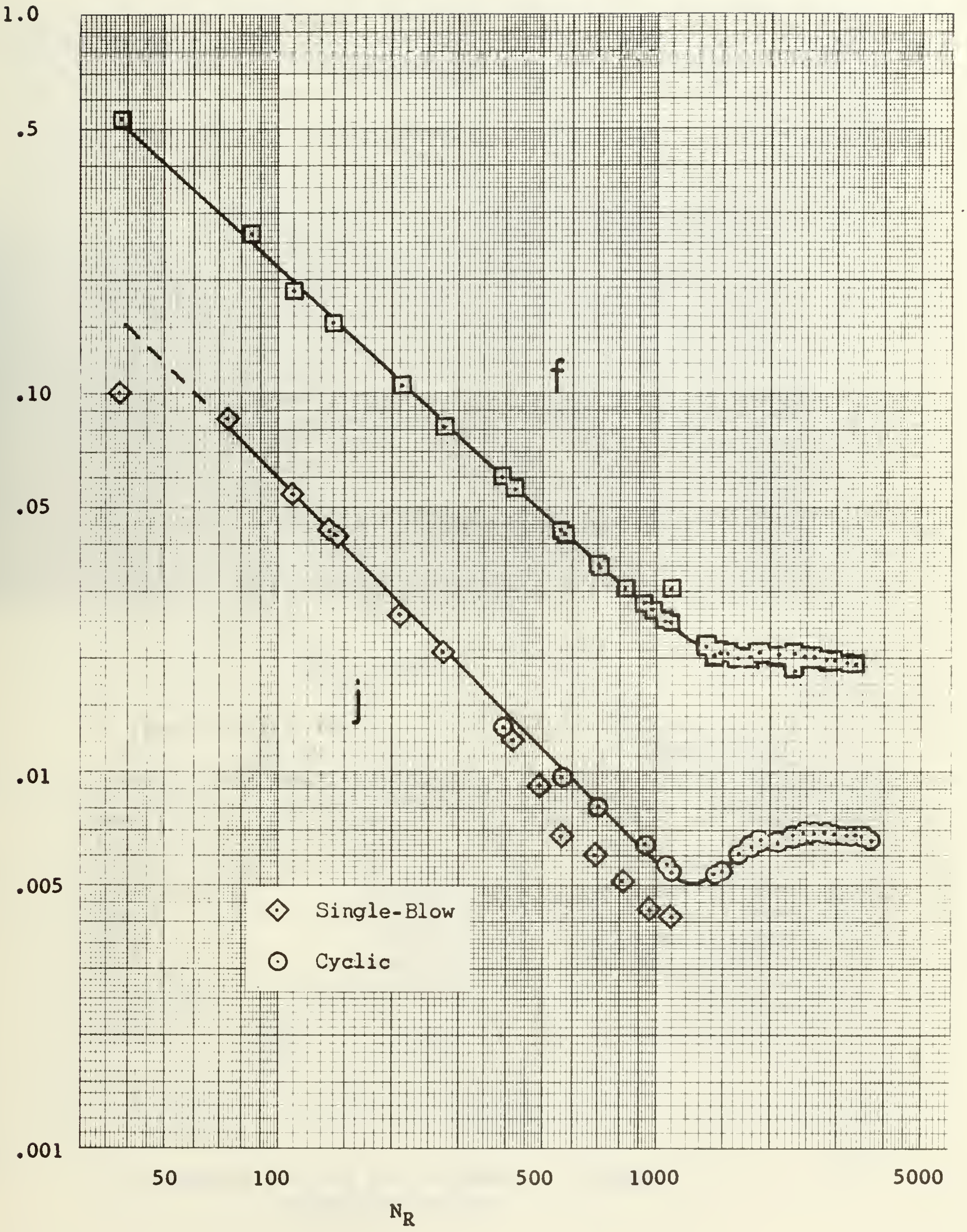

Figure 9. Heat Transfer and Flow Friction Characteristics of Solar No. 2 Matrix.

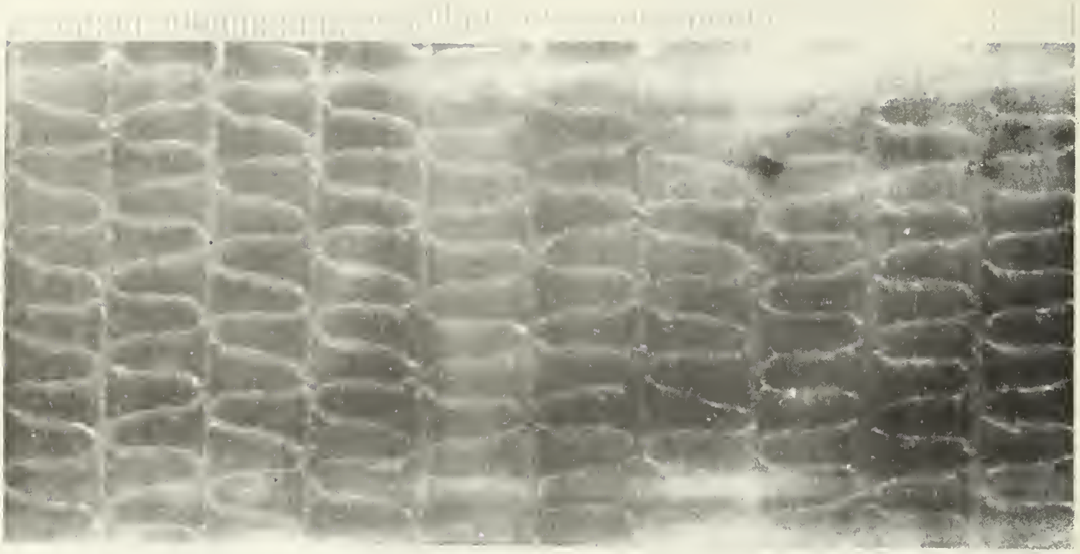

SOLAR # 3

Matrix Material		430 Stainless Steel
Specific Heat, c_s	(Btu/lbm deg F)	.11
Thermal Conductivity, k_s	(Btu/hr ft deg F)	12.8
Material Thickness, a_s	(in)	.005
Total Heat Transfer Area, A	(sq ft)	14.3588
Frontal Area, A_{fr}	(sq ft)	.06803
Conduction Area, A_s	(sq ft)	.01325
Free Flow Area, A_c	(sq ft)	.05478
Matrix Flow Length, L_m	(ft)	.24833
Matrix Volume, V_m	(cu ft)	.01689
Matrix Density, ρ_m	(lbm/cu ft)	94.2656
Compactness, β	(sq ft/cu ft)	849.8962
Porosity, p		.80517
Hydraulic Diameter, D_h	(ft)	.0037895

Figure 10. Geometric and Physical Properties
For Solar #3 Matrix

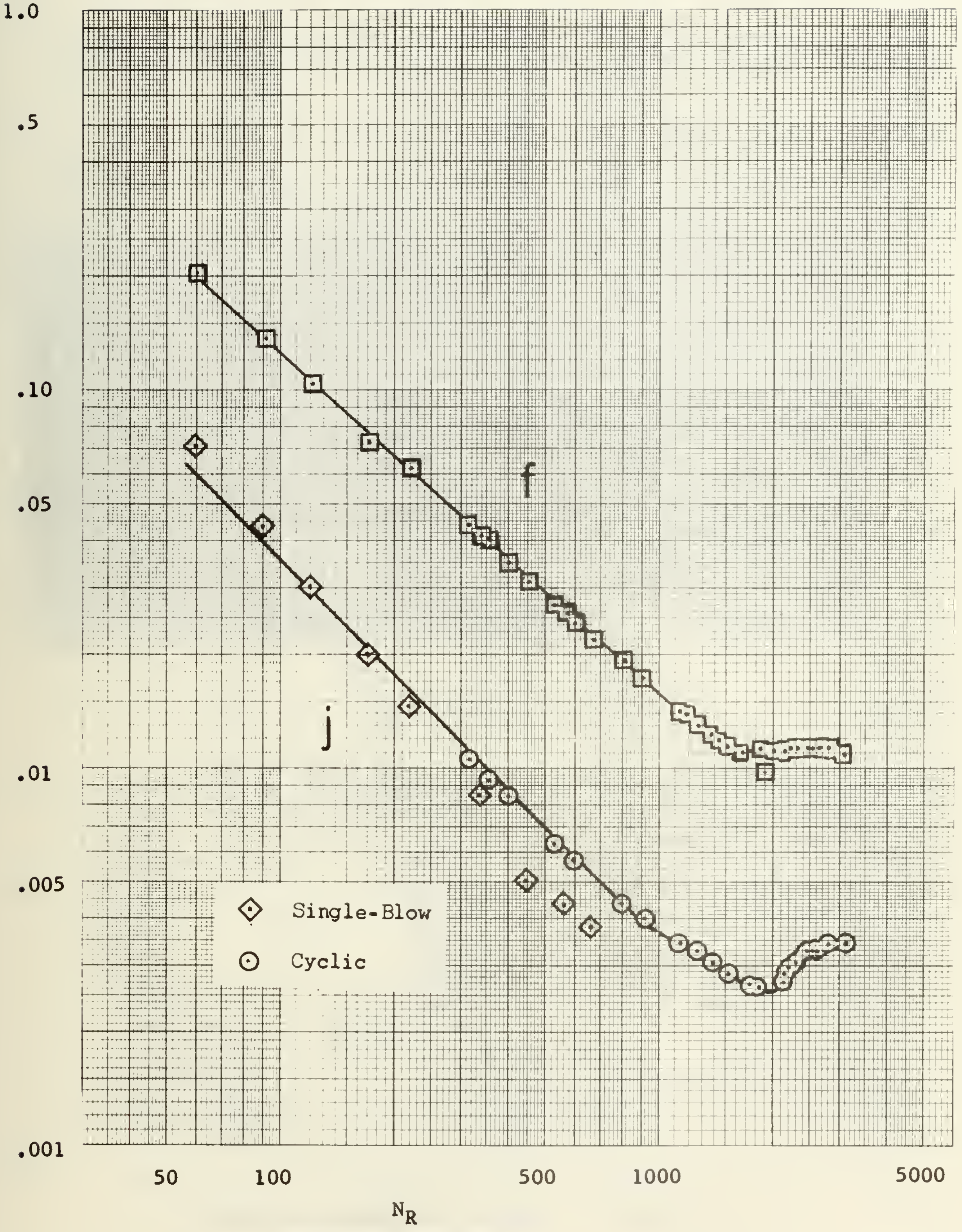

Figure 11. Heat Transfer and Flow Friction Characteristics of Solar No. 3 Matrix.

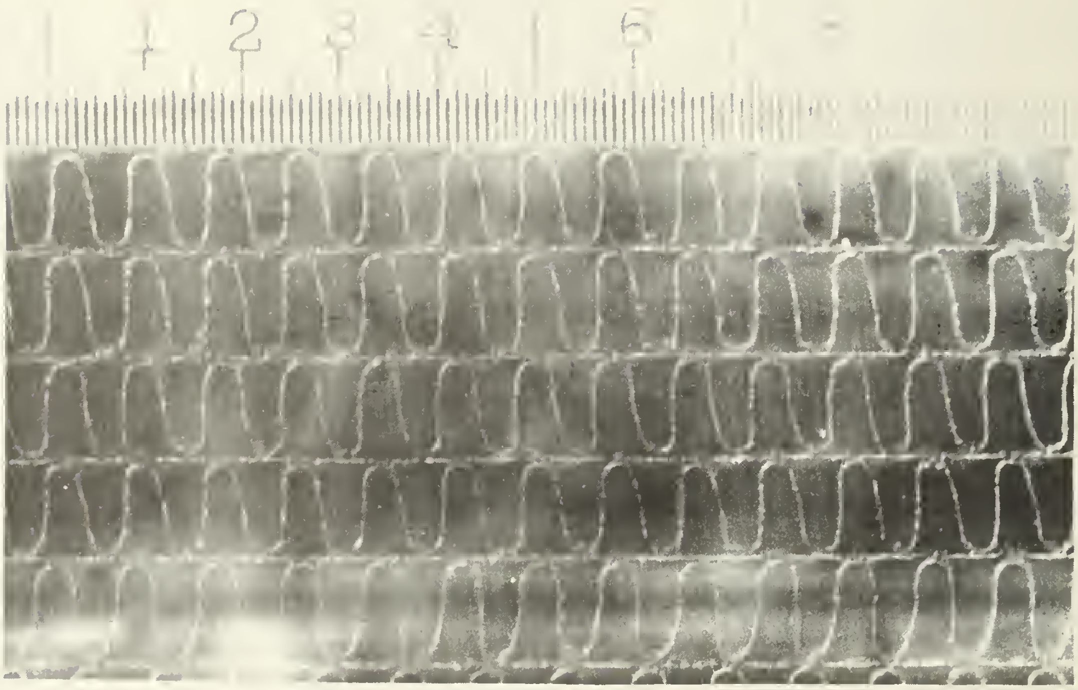

SOLAR # 4

Matrix Material	430 stainless steel	
Specific Heat, c	(Btu/lbm deg F)	.11
Thermal Conductivity, k_s	(Btu/hr ft deg F)	12.8
Material Thickness, a_s	(in)	.005
Total Heat Transfer Area, A	(sq ft)	14.27694
Frontal Area, A_{fr}	(sq ft)	.06713
Conduction Area, A	(sq ft)	.01229
Free Flow Area, A_c	(sq ft)	.05484
Matrix Flow Length, L_m	(ft)	.24417
Matrix Volume, V_m	(cu ft)	.01638
Matrix Density, ρ_m	(lbm/cu ft)	88.5918
Compactness, β	(sq ft/cu ft)	P870.969
Porosity, p		.81690
Hydraulic Diameter, D_h	(ft)	.00375168

Figure 12. Geometric and Physical Properties of Solar #4 Matrix

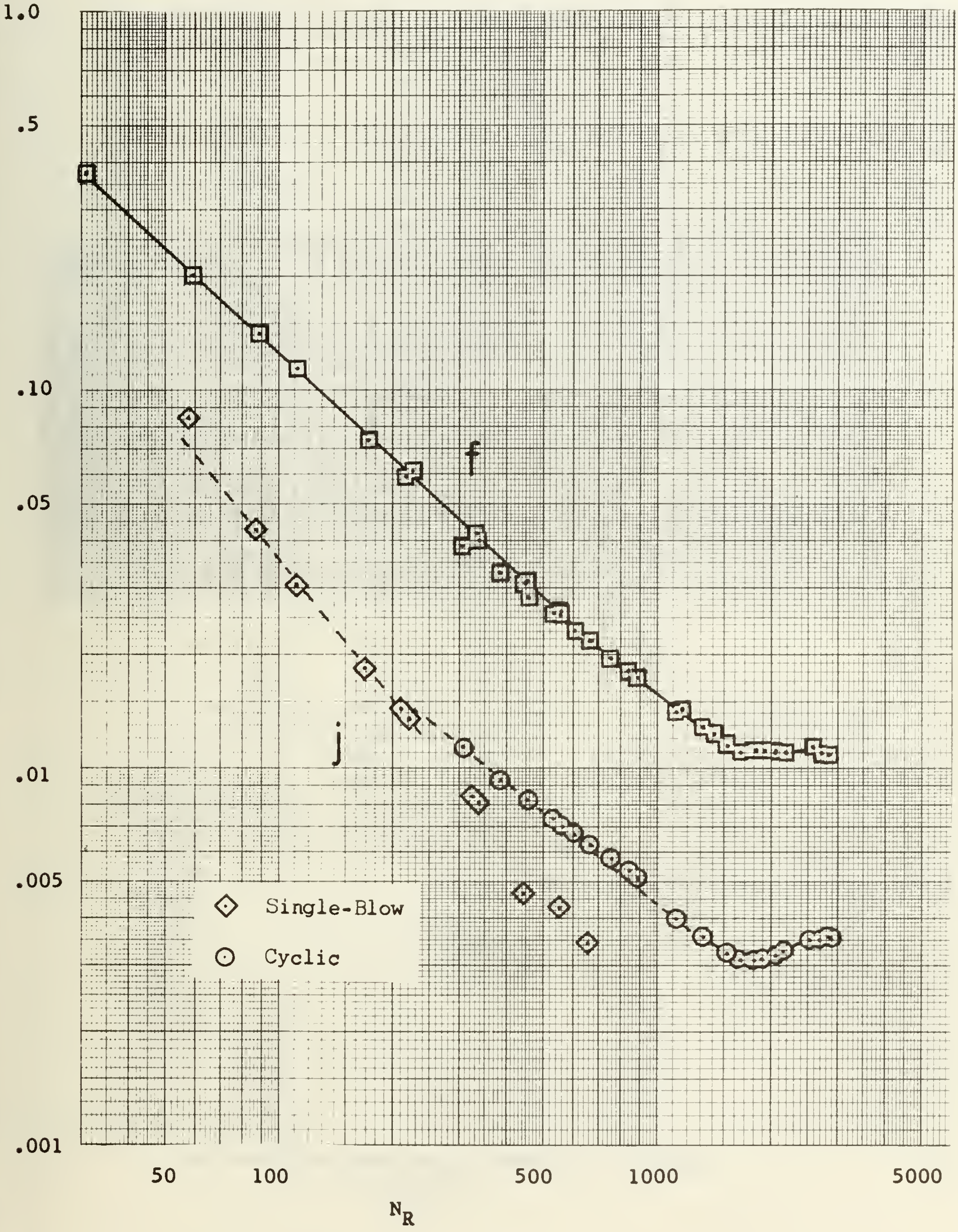

Figure 13. Heat Transfer and Flow Friction Characteristics of Solar No. 4 Matrix.

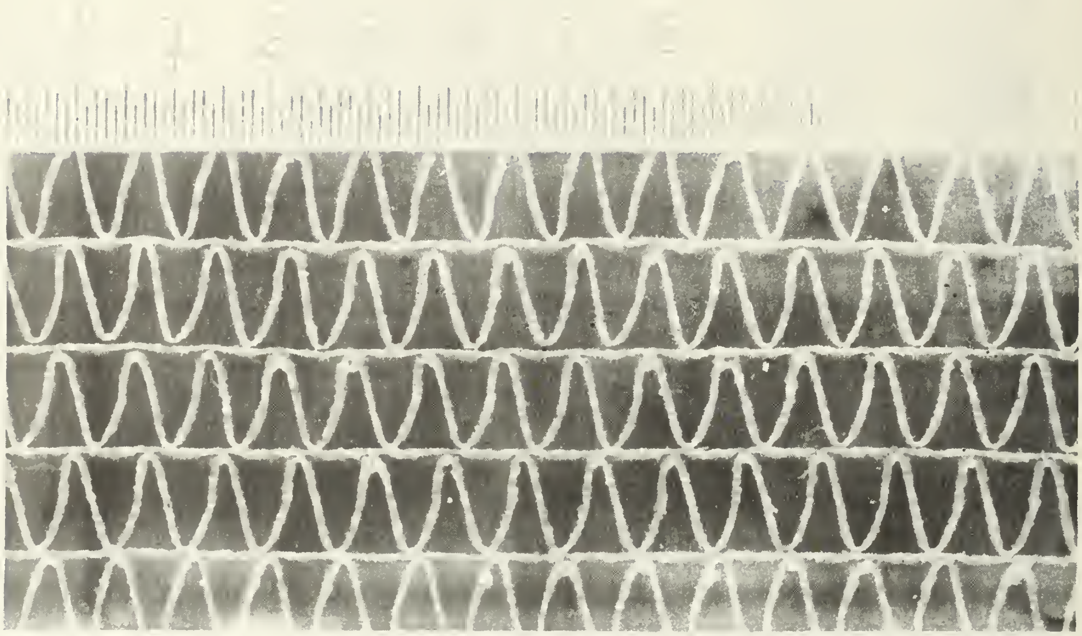

SOLAR # 5

Matrix Material	430 Stainless steel	
Specific Heat, c_s	(Btu/lbm deg F)	.11
Thermal Conductivity, k_s	(Btu/hr ft deg F)	12.8
Material Thickness, a_s	(in)	.005
Total Heat Transfer Area, A	(sq ft)	14.4234
Frontal Area, A_{fr}	(sq ft)	.06781
Conduction Area, A_s	(sq ft)	.01148
Free Flow Area, A_c	(sq ft)	.05633
Matrix Flow Length, L_m	(ft)	.26417
Matrix Volume, V	(cu ft)	.0179
Matrix Density, ρ_m	(lbm/cu ft)	81.9345
Compactness, β	(sq ft/cu ft)	805.13313
Porosity, p		.83066
Hydraulic Diameter, D_h	(ft)	.0041269

Figure 14. Geometric and Physical Properties of Solar #5

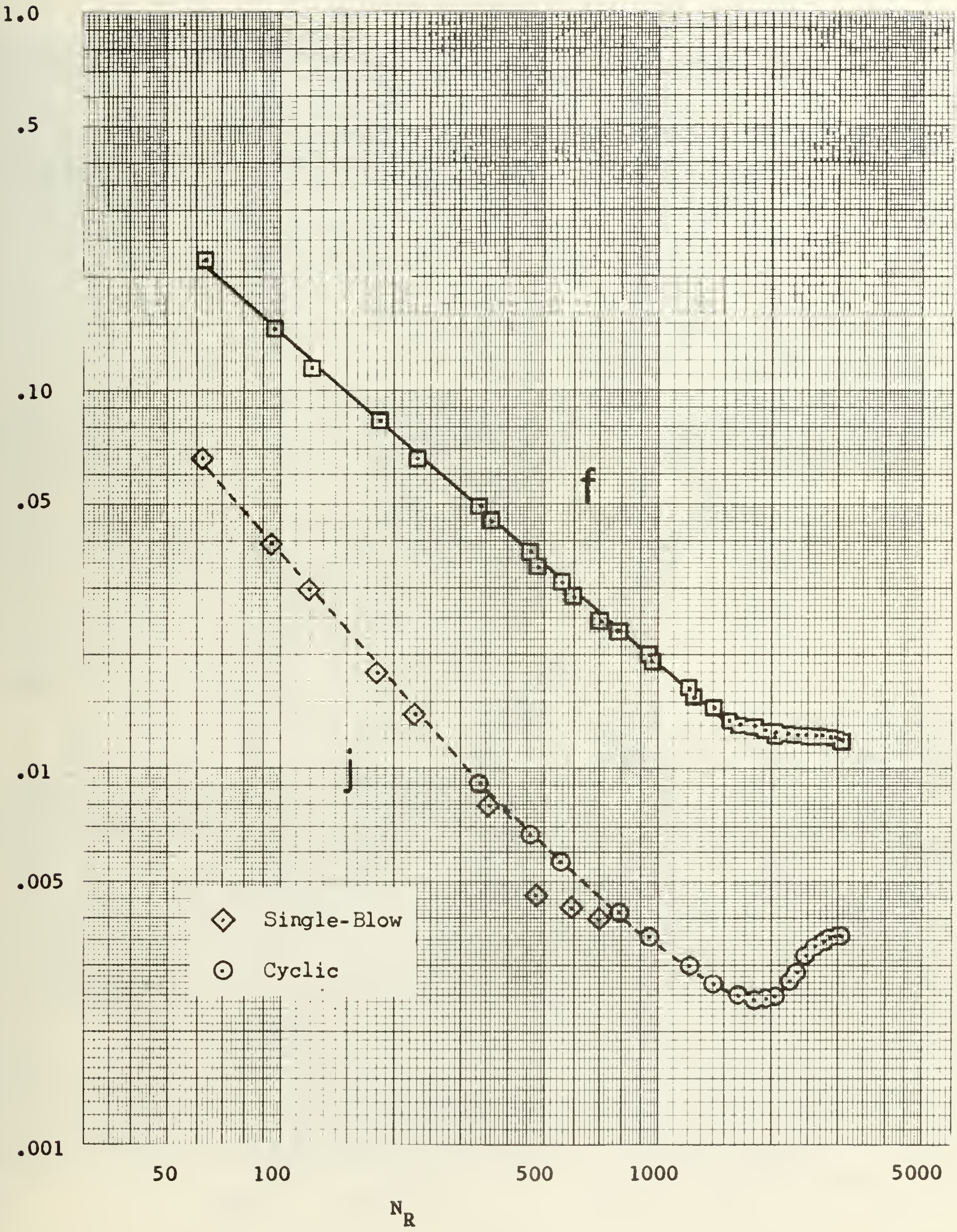

Figure 15. Heat Transfer and Flow Friction Characteristics of Solar No. 5 Matrix.

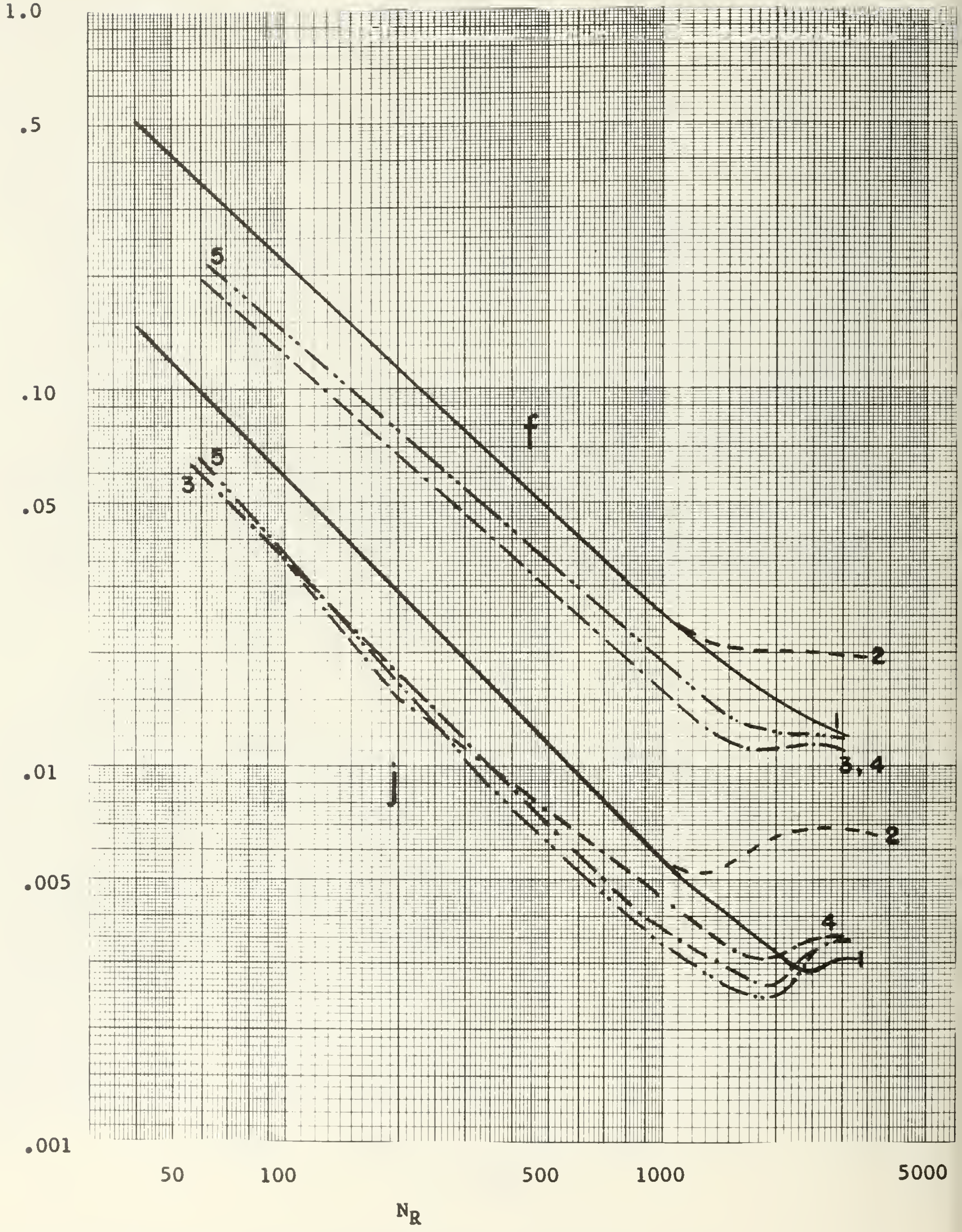

Figure 16. Comparison of Characteristics.

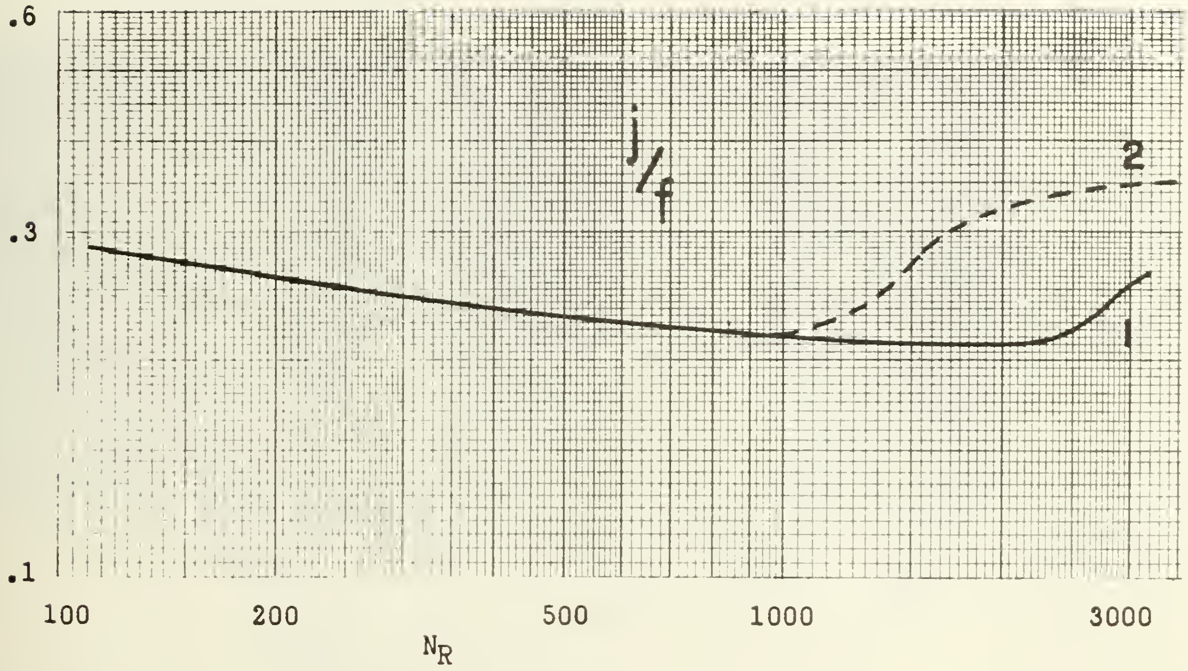

Figure 17. Flow Area Goodness Factors for Solar Nos. 1 and 2 Matrices.

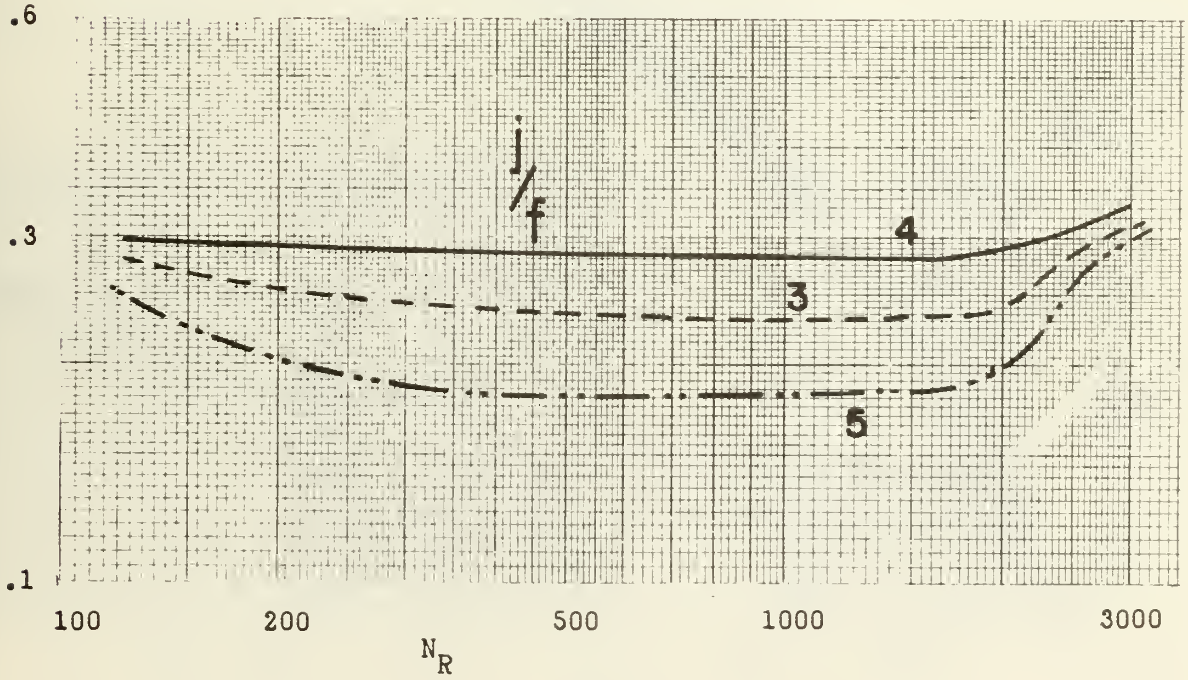

Figure 18. Flow Area Goodness Factors for Solar Nos. 3, 4, and 5 Matrices.

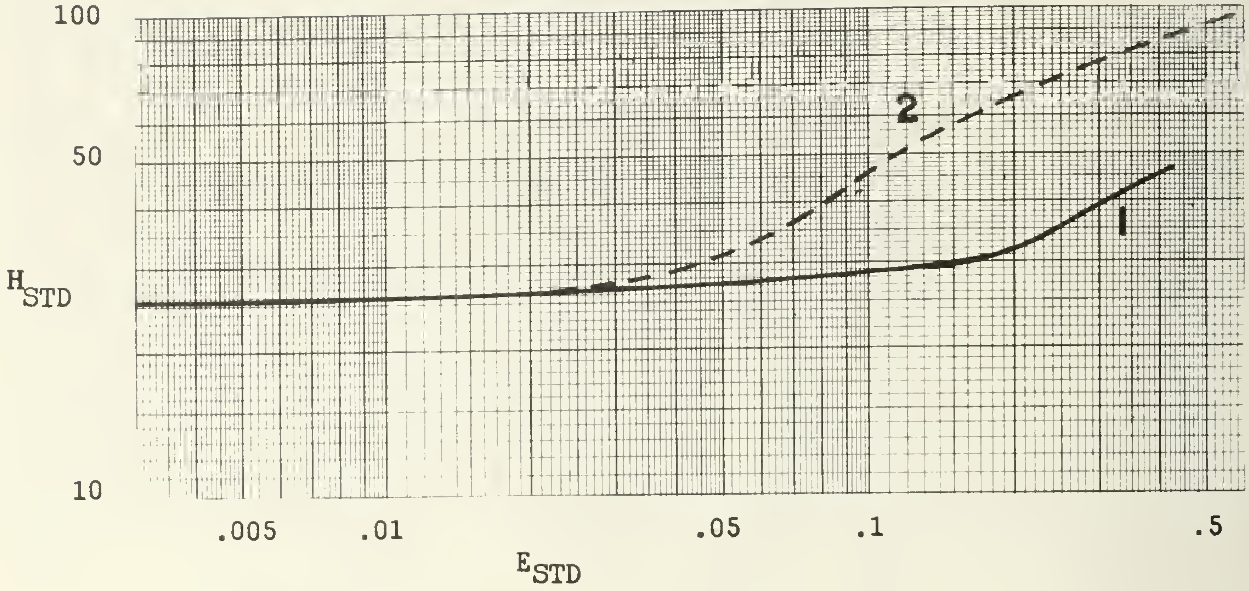

Figure 19. Heat Transfer Power versus Flow Friction Power for Solar Nos. 1 and Matrices.

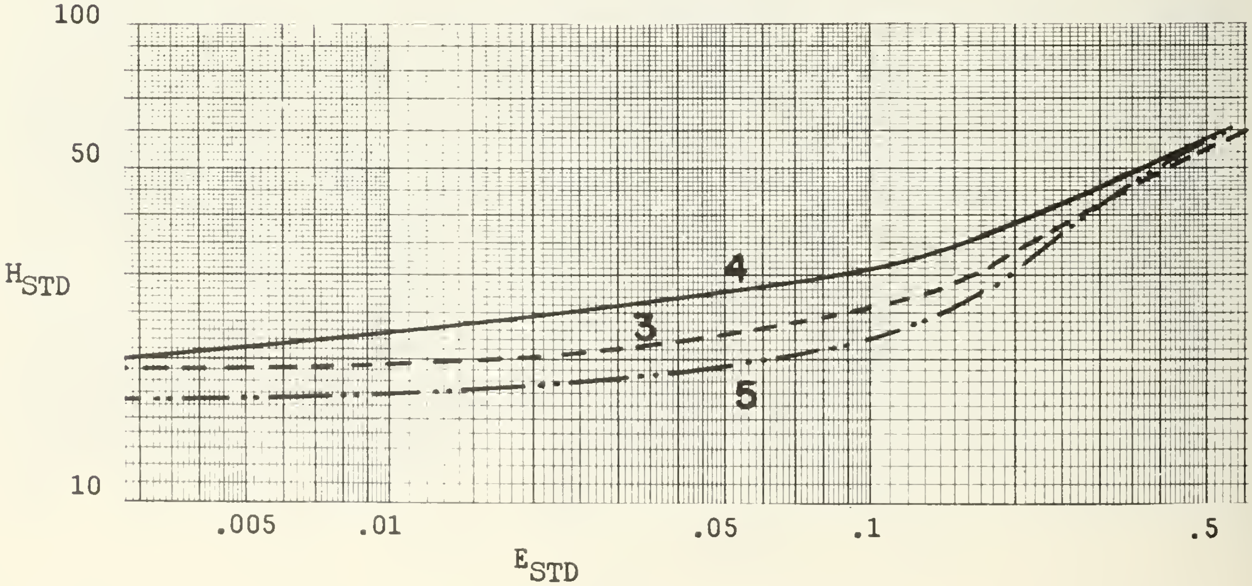

Figure 20. Heat Transfer Power versus Flow Friction Power for Solar Nos. 3, 4, and 5 Matrices.

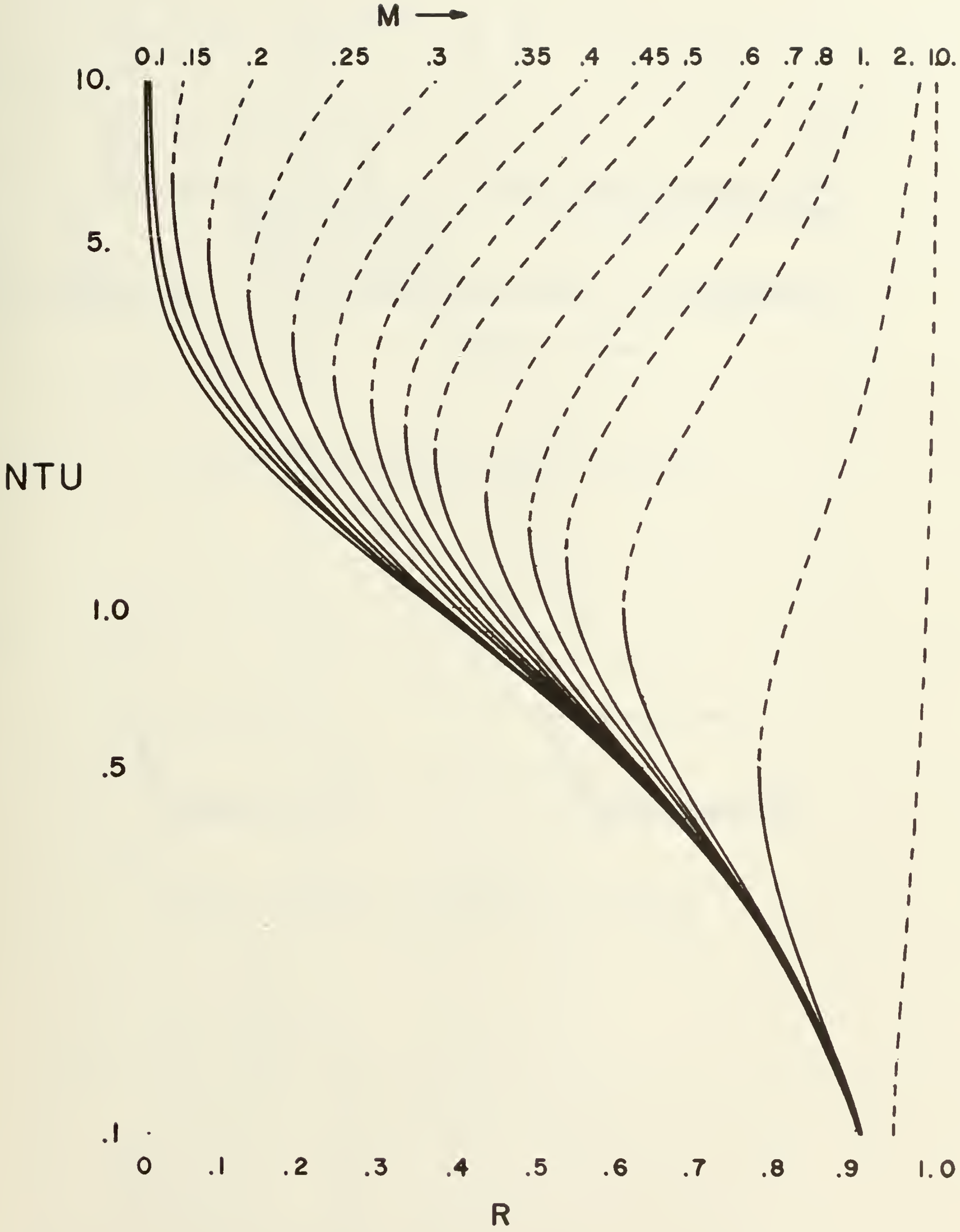

Figure 21. NTU versus Amplitude Ratio.

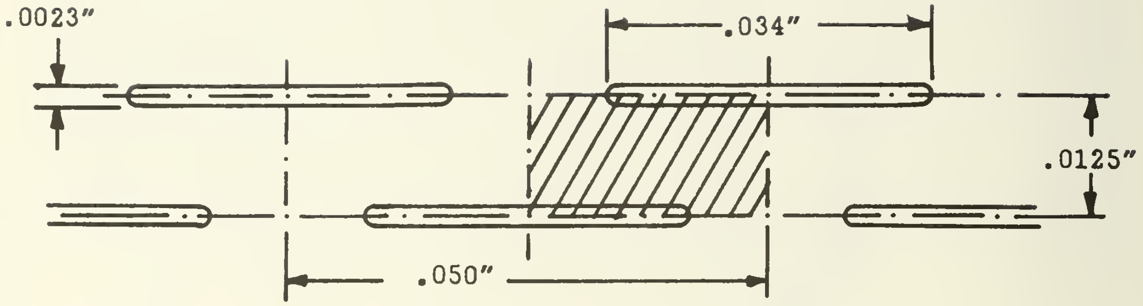

Figure 22. Perforated Nickel Geometry.

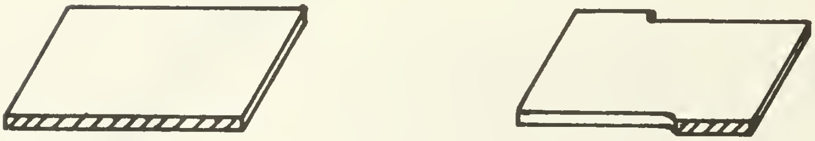

Figure 23. Conduction Parameter Analog.

TABLE I. Summary Description of Matrices

Matrix Desig.	FINS					SPLITTERS		Hydraulic Diameter ft.	$\frac{L}{D_H}$
	Material	thick. in.	per inch	height in.		Material	thick. in.		
Solar #1	Nickel	.005	10	0.10	Sinusoidal	nickel	.005	.00464	64.7
Solar #2	Perforated nickel 80/20 T	.0047	10	0.10	Sinusoidal	nickel	.005	.00463	64.8
Solar #3	430 SS	.005	10	0.10	Sinusoidal maximum fellet braze	430 SS	.005	.00379	79.2
Solar #4	430 SS	.005	10	0.10	Sinusoidal	430 SS	.005	.00375	80.0
Solar #5	430 SS	.005	10	0.10	Triangular (sharp radius)	430 SS	.005	.00413	72.7

TABLE II. Summary of Friction and Heat Transfer Results
Solar #1 Matrix

FRICTION RESULTS		HEAT TRANSFER RESULTS			
FRICTION FACTOR f	REYNOLD'S NUMBER N_R	$N_{St}N_{Pr}^{2/3}$ j	REYNOLD'S NUMBER N_R	NTU	TESTING METHOD
.58553	35.66	.09482	35.14	25.57	S-B
.30134	69.91	.08829	68.89	23.81	S-B
.20595	106.00	.05464	104.47	14.74	S-B
.15680	136.80	.04155	134.83	11.21	S-B
.12574	170.53	.03475	168.08	9.38	S-B
.08867	254.16	.02215	250.50	5.977	S-B
.08029	267.73	.02033	263.87	5.48	S-B
.05971	394.40	.01401	388.72	3.78	S-B
.04418	523.69	.00959	516.15	2.59	S-B
.03663	642.29	.00775	633.05	2.09	S-B
.03713	660.90	.00812	660.90	2.197	CYC
.02736	912.84	.00525	899.71	1.42	S-B
.02419	1060.99	.00536	1060.99	1.449	CYC
.02248	1164.10	.00394	1147.36	1.06	S-B
.02064	1293.89	.00400	1275.26	1.08	S-B
.01995	1346.47	.00430	1346.47	1.162	CYC
.01873	1432.01	.00380	1411.41	1.03	S-B
.01773	1557.13	.00378	1534.71	1.02	S-B
.01652	1676.73	.00358	1676.73	.966	CYC
.01681	1678.22				
.01585	1854.19	.00326	1854.19	.882	CYC
.01486	2024.35	.00309	2024.35	.778	CYC
.01345	2349.97	.00279	2349.97	.754	CYC
.01298	2504.63	.00283	2505.63	.765	CYC
.01265	2660.83	.00293	2660.83	.792	CYC
.01238	2805.05	.00299	2805.05	.807	CYC
.01214	2945.42	.00305	2945.42	.823	CYC
.01202	3040.39	.00308	3040.39	.833	CYC
.01186	3179.90	.00310	3179.90	.837	CYC

TABLE III. Summary of Friction and Heat Transfer Results Solar #2 Matrix

FRICTION RESULTS		HEAT TRANSFER RESULTS			
FRICTION FACTOR	REYNOLD'S NUMBER	$N_{St}N_{Pr}^{2/3}$	REYNOLD'S NUMBER	NTU	TESTING METHOD
f	N_R	j	N_R		
.53389	38.67	.10087	38.12	25.60	S-B
.26494	75.32	.08623	74.24	21.88	S-B
.18811	110.81	.05455	109.21	13.84	S-B
.15304	139.00	.04330	136.98	10.98	S-B
.14937	145.58	.04233	143.48	10.737	S-B
.10594	212.84	.02602	209.78	6.60	S-B
.08185	276.05	.02066	272.04	5.24	S-B
.06003	393.56	.01317	393.56	3.354	CYC
.05593	421.28	.01217	415.24	3.09	S-B
.04840	497.17	.00926	490.02	2.35	S-B
.04383	562.64	.00966	562.64	2.457	CYC
.04258	570.53	.00679	562.26	1.72	S-B
.03559	701.42	.00801	701.42	2.038	CYC
.03521	705.01	.00598	694.80	1.52	S-B
.03072	823.83	.00513	812.02	1.30	S-B
.02798	923.82	.00641	923.82	1.630	CYC
.02720	975.36	.00428	961.25	1.09	S-B
.02510	1064.41	.00572	1064.41	1.453	CYC
.03074	1090.38	.00531	1090.38	1.349	CYC
.02505	1096.74	.00412	1096.74	1.05	S-B
.02142	1368.82				
.02056	1425.27	.00535	1425.27	1.360	CYC
.02078	1479.07	.00545	1479.07	1.385	CYC
.02057	1538.31				
.02005	1639.80	.00602	1639.80	1.531	CYC
.02021	1778.11	.00634	1778.11	1.612	CYC
.02071	1887.96	.00658	1887.96	1.672	CYC
.02057	2098.59	.00671	2098.59	1.704	CYC
.01848	2317.65				
.02046	2318.17	.00679	2318.17	1.726	CYC
.02032	2472.89	.00688	2472.89	1.748	CYC
.02019	2612.20	.00693	2612.20	1.759	CYC
.01995	2821.31	.00693	2821.31	1.760	CYC
.01979	2972.19	.00690	2972.19	1.751	CYC
.01951	3197.52	.00682	3197.52	1.732	CYC
.01934	3355.29	.00679	3355.29	1.724	CYC
.01913	3495.91	.00674	3495.91	1.710	CYC
.01890	3696.46	.00660	3696.46	1.675	CYC

TABLE IV. Summary of Friction and Heat Transfer Results
Solar #3 Matrix

FRICTION RESULTS		HEAT TRANSFER RESULTS			
FRICTION FACTOR	REYNOLD'S NUMBER	$N_{St}N_{Pr}^{2/3}$	REYNOLD'S NUMBER	NTU	TESTING METHOD
f	N_R	j	N_R		
.20320	60.19	.07076	59.32	23.30	S-B
.13761	91.18	.04325	89.87	14.24	S-B
.10327	121.78	.03031	120.03	9.98	S-B
.07288	172.54	.01995	170.06	6.57	S-B
.06223	221.36	.01464	218.18	4.82	S-B
.04422	313.54	.01058	313.54	3.490	CYC
.04132	342.40	.00853	337.48	2.81	S-B
.04015	357.16	.00930	357.16	3.065	CYC
.03507	401.24	.00842	401.24	2.775	CYC
.03125	456.46	.00502	449.90	1.65	S-B
.02705	531.35	.00634	531.35	2.091	CYC
.02574	567.42	.00438	559.26	1.44	S-B
.02427	601.41	.00577	601.41	1.901	CYC
.02200	672.09	.00379	662.44	1.25	S-B
.01938	809.42	.00439	809.42	1.447	CYC
.01737	902.44				
		.00399	917.52	1.316	CYC
.01421	1144.49	.00346	1144.49	1.140	CYC
.01378	1194.66				
.01306	1266.97	.00331	1266.97	1.092	CYC
.01229	1380.58	.00306	1380.58	1.009	CYC
.01193	1436.51				
.01157	1518.23	.00285	1518.23	.940	CYC
.01108	1675.60	.00268	1675.60	.883	CYC
.01123	1858.27	.00263	1858.27	.866	CYC
.00975	1921.60				
.01121	2013.75	.00269	2013.75	.886	CYC
.01123	2141.30	.00285	2141.30	.941	CYC
.01129	2220.69	.00294	2220.69	.970	CYC
.01134	2320.36	.00306	2320.36	1.011	CYC
.01134	2487.33	.00327	2487.33	1.080	CYC
.01134	2544.96	.00330	2544.96	1.089	CYC
.01136	2658.22	.00331	2658.22	1.092	CYC
.01132	2807.06	.00343	2807.06	1.130	CYC
.01099	3091.52	.00342	3091.52	1.126	CYC

TABLE V. Summary of Friction and Heat Transfer Results
Solar #4 Matrix

FRICTION RESULTS		HEAT TRANSFER RESULTS			
FRICTION FACTOR f	REYNOLD'S NUMBER N_R	$N_{St}N_{Pr}^{2/3}$ j	REYNOLD'S NUMBER N_R	NTU	TESTING METHOD
.37693	30.98	.00611	30.53	2.00	S-B
.20381	59.13	.08412	58.28	27.52	S-B
.14272	88.76	.04310	87.49	14.10	S-B
.11402	112.87	.03061	111.25	10.01	S-B
.07412	171.76	.01845	169.30	6.04	S-B
.05929	215.99	.01499	212.89	4.74	S-B
.06105	226.98	.01370	223.71	4.481	S-B
.03866	304.36	.01139	306.36	3.732	CYC
.04174	331.25	.00847	326.48	2.772	S-B
.03983	338.77	.00806	333.91	2.64	S-B
.03290	383.18	.00939	383.18	3.078	CYC
.03100	447.77	.00467	441.35	1.53	S-B
.03139	454.43	.00468	447.88	1.532	S-B
.02881	452.28	.00826	452.28	2.708	CYC
.02566	530.33	.00735	530.33	2.409	CYC
.02546	557.45	.00429	549.45	1.40	S-B
.02616	561.71	.00700	561.71	2.292	CYC
.02309	604.56	.00671	604.56	2.200	CYC
.02172	664.38	.00346	654.85	1.13	S-B
.02142	665.20	.00625	665.20	2.048	CYC
.01958	748.02	.00577	748.02	1.890	CYC
.01820	841.71	.00535	841.71	1.751	CYC
.01741	888.19				
.01756	891.99	.00511	891.99	1.673	CYC
.01441	1120.75	.00398	1120.75	1.303	CYC
.01426	1162.42				
.01291	1303.44	.00358	1303.44	1.173	CYC
.01239	1415.34				
.01156	1526.00	.00324	1526.00	1.062	CYC
.01103	1668.92	.00312	1668.92	1.020	CYC
.01126	1807.14	.00310	1807.14	1.015	CYC
.01116	1904.64	.00313	1904.64	1.025	CYC
.01161	1908.14				
.01107	2041.42	.00321	2041.42	1.072	CYC
.01106	2170.84	.00327	2170.84	1.102	CYC
.01156	2557.98	.00350	2557.98	1.144	CYC
.01095	2711.58	.00351	2711.58	1.148	CYC
.01088	2828.75	.00356	2828.75	1.165	CYC
.01086	2887.46	.00358	2887.46	1.172	CYC

TABLE VI. Summary of Friction and Heat Transfer Results Solar #5 Matrix

FRICTION RESULTS		HEAT TRANSFER RESULTS			
FRICTION FACTOR	REYNOLD'S NUMBER	$N_{St}N_{Pr}^{2/3}$	REYNOLD'S NUMBER	NTU	TESTING METHOD
f	N_R	j	N_R		
.22228	63.05	.06573	62.15	21.15	S-B
.14597	96.54	.03924	95.15	12.62	S-B
.11431	121.54	.02967	119.79	9.54	S-B
.08385	183.46	.01805	180.83	5.81	S-B
.06594	231.11	.01393	227.80	4.48	S-B
.04962	337.08	.00921	337.08	2.972	CYC
.04488	360.72	.00800	355.54	2.57	S-B
.03749	458.12	.00670	458.12	2.160	CYC
.03439	482.55	.00460	475.63	1.48	S-B
.03123	556.72	.00568	556.72	1.831	CYC
.02846	600.21	.00426	591.59	1.37	S-B
.02472	708.74	.00396	698.57	1.28	S-B
.02298	788.74	.00418	788.74	1.347	CYC
.01993	949.26	.00355	946.26	1.145	CYC
.01907	964.34				
.01637	1203.37	.00301	1203.37	.970	CYC
.01548	1247.65				
.01466	1405.06	.00268	1405.06	.862	CYC
.01341	1548.85				
.01320	1635.14	.00250	1635.14	.804	CYC
.01304	1804.55	.00243	1804.55	.783	CYC
.01272	1938.77	.00247	1938.77	.794	CYC
.01207	2040.53				
.01252	2061.91	.00249	2061.91	.802	CYC
.01235	2214.46	.00272	2214.46	.874	CYC
.01233	2323.94	.00289	2323.94	.932	CYC
.01222	2480.71	.00319	2480.71	1.028	CYC
.01218	2622.09	.00337	2622.09	1.086	CYC
.01212	2736.70	.00343	2736.70	1.104	CYC
.01208	2876.26	.00353	2867.26	1.135	CYC
.01204	2966.69	.00356	2966.69	1.145	CYC
.01198	3028.94	.00359	3028.94	1.155	CYC
.01198	3069.59	.00361	3069.59	1.162	CYC

APPENDIX A

The cyclic technique employed is that described by Bell and Katz (5). The assumptions made in the analysis are:

(1) All cross sections of the solid normal to some fixed direction are uniform.

(2) The gas velocity is uniform throughout the passage.

(3) The physical properties of the gas and of the specimen are constant.

(4) The surface heat-transfer coefficient is constant.

(5) The inlet gas temperature varies sinusoidally. Bell and Katz have found solutions to the problem under the following three alternative assumptions:

(a) The thermal conductivity in the solid is infinite.

(b) The thermal conductivity in the solid is zero in the longitudinal (flow) direction and infinite in the transverse direction.

(c) The thermal conductivity in the solid is zero in the longitudinal direction and finite in the transverse direction.

Of the three solutions, that of case (b) is most nearly satisfied in the case of high mass flow rates with its low values of conduction parameter. A summary of the theory for this case is presented below:

Case (b) - Solid having infinite transverse and zero longitudinal conductivity.

Energy balance:

Fluid: $$\dot{m}c_p\left(\frac{\delta tf}{\delta x}\,dx + \frac{\delta tf}{\delta \Theta}\,d\Theta\right) = hb(t_f - t_s)\,dx \qquad \text{(A-1)}$$

Solid: $$\rho_s A_s L_s \frac{\delta ts}{\delta \Theta}\,dx = hb(t_f - t_s)\,dx \qquad \text{(A-2)}$$

Inlet and Initial Conditions:

Inlet: $t_f(0,\Theta) = t_m + \Delta \sin \omega_\circ \Theta$ (A-3)

Initial: $t_s(0) = t_{so}$ (A-4)

Initial: $t_f(x,0) = t_o(x)$ (A-5)

where Δ is the peak amplitude of the sinusoidally varying temperature and t_m is some suitable mean temperature. Introducing the following dimensionless parameters:

(1) Time $\bar{\tau} = \frac{u\Theta}{L}$

(2) Position $\xi = \frac{x}{L}$

(3) Frequency $\omega = \frac{\omega_\circ L}{u}$

(4) Flow: $M = \frac{\dot{m}\ c_p}{W s C s \omega}$

(5) Heat transfer units $Ntu = \frac{hA}{\dot{m} c_p}$

where:

u = flow velocity (ft/sec)

Θ = time (sec)

L = matrix flow length (ft)

x = distance from matrix inlet in direction of flow (ft)

$\omega_\circ$ = angular frequency of temperature oscillation (rad/sec).

Introducing the above dimensionless parameters into (A-1) through (A-5) and rearranging yields:

Fluid: $\frac{\delta t_f}{\delta \xi} + \frac{\delta t_f}{\delta \tau} + Ntu(t_f - t_s) = 0$

Solid: $\frac{\delta t_s}{\delta \bar{\tau}} - M\ \omega\ Ntu(t_f - t_s) = 0$

Inlet: $t_f(0,\bar{\tau}) = t_{so} + \Delta \sin \omega\bar{\tau}$

Initial: $t_s(0) = t_{so}$

Initial: $t_f(\xi,0) = t_o(\xi)$

This system has the periodic solution:

$$t_f(\xi,\bar{\tau}) = t_m + \Delta e^{-\alpha\xi} \sin(\omega\bar{\tau} + \Omega\xi)$$

$$t_s(\xi,\bar{\tau}) = t_m + \Delta\alpha e^{-\alpha\xi}[M\ Ntu \sin(\omega\tau - \Omega\xi) - \cos(\omega\tau - \Omega\xi)]$$

where:

$$\alpha = Ntu/[1 + (M\ Ntu)^2]$$

$$\Omega = M(Ntu)^2/[1 + (M\ Ntu)^2] + \omega$$

The ratio of the inlet temperature amplitude to the exit temperature amplitude is

$$R = e^{-\left[\frac{Ntu}{1 + (M\ Ntu)^2}\right]} \tag{A-6}$$

This relationship is plotted in Figure 25 as Ntu versus R for various values of M.

The solutions for the ratio of temperature amplitudes for cases (a) and (c) are presented below:

Case (a). Infinite conductivity in solid.

$$R = \left[\frac{e^{-2Ntu} + M^2(1 - e^{-Ntu})^2}{1 + M^2\ (1 - e^{-Ntu})^2}\right]^{\frac{1}{2}}$$

This solution is an approximation to a Taylor series around $\omega = 0$ when NTU < 2.0.

Case (c). Solid having finite transverse and zero longitudinal conductivity.

$$R = \exp\left\{- \frac{Ntu}{1+(M\ Ntu)^2} \left[1 + \frac{\sigma^2 M\ Ntu\ (M^2 Ntu^2 - 1)}{6(1 + M^2\ Ntu^2)} + \dots\right]\right\}$$

where:

$\sigma^2 = \omega_o as\ C_s\ \rho_s/2ky$

as = plate thickness

ky = thermal conductivity in transverse direction

This solution coincides with the value found for R for case (b) whenever the series in σ can be approximated satisfactorily by its first term. For a more detailed explanation on the solutions for the preceding three cases the reader is referred to reference (11). For the treatment of the three cases utilizing a liquid as the fluid the paper written by Chastain (12) should be consulted.

On the use of the three solutions, Bell and Katz have shown that the ratio of the two amplitude ratios found for cases (a) and (b) are coincident when $M < 0.1$ and $NTU \approx 1.0$. In the experimental work performed by Bell and Katz, the ratio of the two amplitude ratios determined for cases (a) and (c) was found to be within 1% of unity. Thus, if the experimental values of M are selected near 0.1, and the resulting NTU's near unity, no serious error is introduced by assuming zero thermal conductivity in the longitudinal (flow) direction, and employing the solution for case (b).

APPENDIX B

Data Reduction Relationships

The relationships presented in this appendix were used to calculate the heat transfer and flow friction characteristics of the matrices tested.

Geometry

The three most significant geometric parameters that provide a means of comparison between matrices are so defined that there exists a unique relation between them. Determination of any two of the following fixes the third:

(1) Hydraulic diameter

$$D_h = 4r_h = \frac{4 \text{ x free flow area}}{\text{heat transfer area}} = 4\frac{Ac}{A}\,L \tag{B-1}$$

(2) Porosity

$$p = \frac{\text{free flow area}}{\text{frontal area}} = \frac{Ac}{A_{fr}} \tag{B-2}$$

(3) Area Compactness

$$\beta = \frac{\begin{array}{c}\text{total}\\ \text{transfer surface area}\end{array}}{\text{total volume}} = \frac{A}{A_{fr}L} \tag{B-3}$$

If (B-2) is divided by (B-3) the previous interdependency results:

$$r_h = \frac{p}{\beta} \tag{B-4}$$

Maximum Slope

The maximum slope of the generalized cooling curve is a function of NTU and λ [4].

$$\left[\frac{d\left(\frac{t_{f2} - t_i}{t_{f1} - t_i}\right)}{d\left(\frac{\tau}{Ntu}\right)}\right]_{max} = \varphi\,(Ntu, \lambda)$$

where:

τ = generalized time variable, t_i = initial matrix temp.

$\tau = \frac{hA}{WsCs}\,\Theta$ t_{f1} = air temp. upstream of matrix, $\Theta > 0$

$Ntu = \frac{hA}{\dot{m}c_p}$ t_{f2} = air temp. downstream of matrix

Therefore:

$$\frac{\tau}{Ntu} = \frac{\dot{m}c_p}{W_sC_s}\,\Theta \qquad \text{(B-5)}$$

Furthermore:

$$\frac{t_{f2} - t_i}{t_{f1} - t_i} = \frac{t_{f2} - t_{f1}}{t_{f1} - t_i} + 1$$

and:

$$d\left(\frac{t_{f2} - t_i}{t_{f1} - t_i}\right) = \left(\frac{1}{t_{f1} - t_i}\right) d\;(t_{f2} - t_{f1}) \qquad \text{(B-6)}$$

combining (B-5) and (B-6)

$$\frac{d\left(\frac{t_{f2} - t_i}{t_{f1} - t_i}\right)}{d\left(\frac{\tau}{Ntu}\right)} = \frac{WsCs}{mc_p} \cdot \frac{1}{t_{f1} - t_i} \cdot \frac{d(t_{f2}-t_{f1})}{d\Theta} \qquad \text{(B-7)}$$

considering the following sketch of a generalized cooling curve:

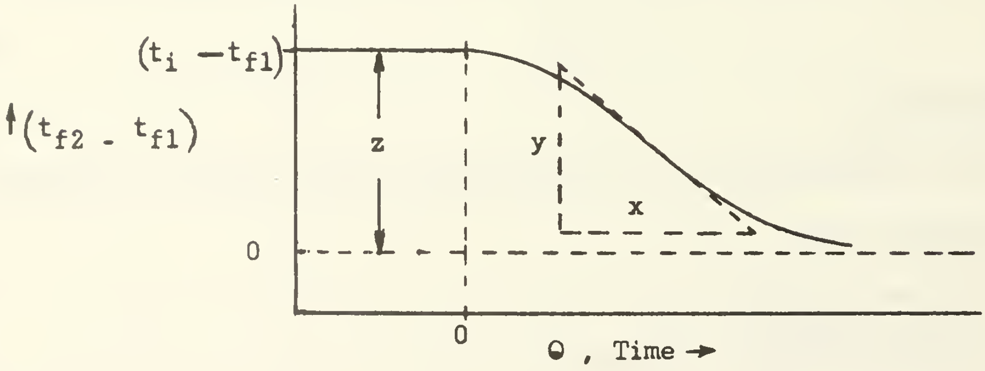

$$\frac{d(t_{f2} - t_1)}{d\Theta} = \left|\frac{Y}{X}\right|$$

$$\frac{x}{\text{chart speed}} = d\Theta$$

$$d(t_{f2} - t_{f1}) = Y$$

$$(t_i - t_{f1}) = Z$$

combining the above measured and recorded quantities with

$$\frac{W_sC_s}{\dot{m}c_p} = \frac{\text{matrix heat capacity}}{\text{fluid heat capacity}} = \frac{\bar{C}_s}{C_f}\ \text{sec}^{-1}$$

and equation (B-7), yields:

$$\left[\frac{d\left(\frac{t_{f2} - t_i}{t_{f1} - t_i}\right)}{d\left(\frac{\tau}{Ntu}\right)}\right] = \frac{\bar{C}_s}{C_f}\ \frac{1}{Z}\ \frac{Y}{X} \tag{B-8}$$

with this value of maximum slope and $\lambda = \dfrac{k_sA_s}{\dot{m}c_p}$

enter Table 1 or Figure 3 of Ref. [2] to obtain the corresponding value of NTU.

Cyclic Relationships

The cyclic tests were made at the higher mass flow rates where case (b) of Appendix A is most nearly satisfied. For this case

$$R = \exp\left[-\frac{Ntu}{1 + (M\ Ntu)^2}\right] \tag{B-9}$$

Solving (B-9) for NTU, we obtain two possible solutions

$$NTU = \frac{1 \pm \sqrt{1 - (2\ M\ \ln 1/R)^2}}{2\ M^2\ \ln 1/R} \tag{B-10}$$

As discussed by Bell and Katz [5], only the smaller magnitude solution has physical meaning. Hence

$$NTU = \frac{1 - \sqrt{1 - (2M\ \ln 1/R)^2}}{2\ M^2\ \ln 1/R} \tag{B-11}$$

A plot of equation (B-10) is shown in Figure 25. The solid line portion of the constant M curves represent equation (B-11).

Mass Flow Rate

The mass flow rate, $\dot{m}$, was calculated in accordance with references (7) and (8):

$$\dot{m} = 359 K d_o^2 FaY \sqrt{\Delta P_o \gamma} \quad (\text{lbm/hr}) \qquad \text{(B-12)}$$

where

K = flow coefficient, including velocity of approach factor

$= \dfrac{C}{\sqrt{1 - \bar{\beta}^4}}$ with C = orifice coefficient of discharge (20)

and $\bar{\beta}$ = ratio of orifice diameter to internal pipe diameter,

d_o = orifice diameter, inches

Fa = thermal expansion factor for orifice plate

Y = expansion factor of fluid

γ = specific weight of fluid flowing $= \dfrac{P}{RT}$

with P = absolute static pressure at orifice (lb/ft^2)

R = 53.3 ($\text{ft-lb}_f/\text{lb}_m$-°R), universal gas constant for air

$T = [t_o(°\text{F}) + 459.7]$ °R , abs. temp at orifice

ΔP_o = pressure drop across the orifice (in. H_2O)

making the substitution of $K = \dfrac{C}{\sqrt{1 - \bar{\beta}^4}}$ and $\gamma = \dfrac{P}{RT}$, since the magnitude of the local acceleration of gravity, g, is taken as being equal to the magnitude of standard acceleration, gc, into (B-12) yields:

$$\dot{m} = 359 \frac{C}{\sqrt{1 - \bar{\beta}^4}} \quad d_o^2 \sqrt{\Delta P_o \frac{P}{RT}} \ (FaY) \qquad \text{(B-13)}$$

From reference (7), Figure 40A

$$Y = 1 - (0.41 + 0.35\ \bar{\beta}^4)\ \frac{x}{k}$$

where k = ratio of specific heats for air = 1.4

$$x = \frac{\Delta P_o \text{(in. Hg abs.)}}{P \text{ (in. Hg abs.)}}$$

and from Figure 38 of same reference

$Fa = 1.0$

also:

$$P = (Patm - \frac{P_o}{13.6})\ .4912 \times 144\ (lbf/ft^2)$$

where:

Patm is the local atmospheric pressure (in. Hg)

P_o is the static pressure upstream of the orifice plate (in. Hg)

Inserting into (B-13) the required numerical constants to make the equation dimensionally consistent and the above defined values or relationships for P, T, Y, x, k, R and F_a, (B-13) becomes:

$$\dot{m} = 589.81 \frac{C}{\sqrt{1 - \beta^4}}\ d_o^2\ [1 - (.41 + .35\beta^4) \frac{\Delta Po}{(Patm - \frac{Po}{13.6})\ 99.02}\ ] \left[\frac{\Delta Po(Patm - \frac{Po}{13.6}}{t_o + 459.7}\right]^{\frac{1}{2}} \tag{B-14}$$

Reynold's Number

By definition:

$$N_R = \frac{D_h G}{\mu} \tag{B-15}$$

where G is the mass flow velocity based on the free flow area, Ac

$$G = \frac{\dot{m}}{Ac} = \frac{\dot{m}}{p\ Afr} \tag{B-16}$$

substituting (B-15) into (B-16):

$$N_R = \frac{\dot{m}}{\mu Afr} \cdot \frac{D_h}{p} \qquad \text{from (B - 4)}\ \frac{r_h}{p} = \frac{1}{\beta}$$

therefore:

$$N_R = (\frac{4\ \dot{m}}{\mu Afr})\ (\frac{1}{\beta}) \tag{B-17}$$

For ease of calculation, substitute (B-3), $\beta = \frac{A}{Af_r L}$

into (B-17)

$$N_R = \frac{4\dot{m}L}{A\mu} \tag{B-18}$$

Fanning Friction Factor

The following sketch depicts the flow system to be considered:

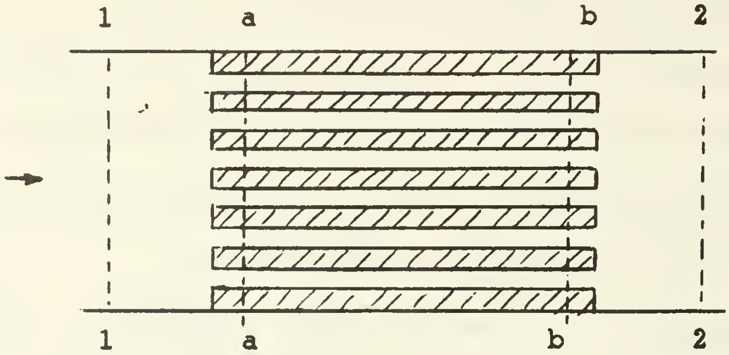

For a gas flow heat exchanger, the pressure changes from section 1 to a and from b to 2 are very small relative to the total pressure, therefore the specific volumes $v_a \approx v_1$, and $v_b \approx v_2$. Since testing is performed with air at moderate pressure, the perfect gas law is applicable.

The relation for the flow stream pressure drop calculation for most heat exchanger cores is (10)

$$\frac{\Delta P}{P_1} = \frac{G^2}{2g_c}\,\frac{v_1}{P_1}\left[\underbrace{(K_c + 1 - p^2)}_{\text{entrance effect}} + \underbrace{2\left(\frac{v_2}{v_1} - 1\right)}_{\text{flow acceleration}} + \underbrace{f\,\frac{A}{Ac}\,\frac{vm}{v_1}}_{\text{core friction}} \underbrace{- (1 - p^2 - Ke)\,\frac{v_2}{v_1}}_{\text{exit effect}}\right] \tag{B-19}$$

Solving (B-19) for f in the isothermal case and recalling from (B-1) that $\frac{A}{Ac} = \frac{L}{r_h}$ also $v = \frac{1}{\rho}$

$$f = \left[2g_c\rho_m\,\frac{\Delta P}{G^2} - \left(\frac{Kc}{P_1} + \frac{Ke}{P_2}\right)\frac{P_1 + P_2}{2} + \frac{P_1 + P_2}{2}\left(\frac{1}{\rho_2} - \frac{1}{\rho_1}\right)(1+p^2)\right]\frac{r_h}{L} \tag{B-20}$$

where $\rho m = \frac{\rho_1 + \rho_2}{2}$ with the upstream values subscripted by 1 and the downstream by 2. Kc is the entrance coefficient and Ke the exit coefficient, both depend on porosity, geometry of the flow cross section, and matrix Reynolds' number [9]. Since the ultimate method of calculating all values for this report was by digital computer, the analytical expressions defined and formulated by Kays in reference [9] were utilized.

(1) Contraction ratio, $C_c = 0.611 + .045p + .344\, p^{5.7}$ (B-21)

(2) Velocity distribution factor, Kd

(a) circular tubes

laminar flow

$Kd = 1.333$

turbulent flow

$f = 0.049\, N_R^{-.2}$ (Fanning friction factor, circular tubes)

$$Kd = 1.09068\,(4f) + 0.0588\sqrt{4f} + 1 \qquad \text{(B-22)}$$

(b) gap, laminar and turbulent

$$\frac{Kd\ (\text{gap}) - 1}{Kd\ (\text{circular}) - 1} = 0.6$$

(c) square, laminar and turbulent

$$\frac{Kd\ (\text{square}) - 1}{Kd\ (\text{circular}) - 1} = 1.17$$

(d) triangle, laminar and turbulent

$$\frac{Kd\ (\text{triangle}) - 1}{Kd\ (\text{circular}) - 1} = 1.29$$

When utilizing the appropriate Kd for the core under evaluation and for the existing type of flow,

$$\text{Exit coefficient} \quad Ke = 1 - 2Kdp + p^2 \qquad \text{(B-23)}$$

$$\text{Entrance coefficient:} \quad Kc = \frac{1 - 2Cc + C_c^2(2Kd-1)}{C_c^2} \qquad \text{(B-24)}$$

Considering an order of magnitude approximation, the first term in the brackets in (B-20) is the greatest contributor to the friction factor for small pressure differentials.

Therefore, the approximation that

$$\frac{P_1 + P_2}{2} \approx Pm \approx P_1 \approx P_2$$ reduces (B-20) to

the following

$$f = \left[2gc\rho m \frac{\Delta P}{G2} - (Kc + Ke) - \frac{\Delta P}{Pm}(1+p^2)\right]\frac{r_h}{L} \qquad \text{(B-25)}$$

It is evident from (B-25) that:

$$f \approx 2gc\ \rho m\ \frac{\Delta P}{G^2}\ \frac{r_h}{L},\ 4r_h = p/\beta \text{ and } G = \dot{m}/p^{A}fr$$

$$f \approx 2gc\ \rho m\ \Delta P\left(\frac{Afr^2}{4Lm^2}\right)\left(\frac{p^3}{\beta}\right)$$

therefore for a given matrix

$$f\alpha\ p^3/\beta$$

Colburn Factor

Colburn-j factor is defined as:

$$j = Nst\ N_{pr}^{2/3} = \frac{h}{Gc_p}\ Npr^{2/3} \qquad \text{(B-26)}$$

Substituting (B-16) for G and multiplying $\frac{A}{A}$ yields:

$$j = \frac{hA}{mc_p} \cdot \frac{Ac}{A} \cdot N_{pr}^{2/3}, \quad \text{but NTU} = \frac{hA}{\dot{m}c_p}$$

therefore:

$$j = NTU\ \frac{Ac}{A}\ N_{pr}^{2/3},$$ combining equations (B-1)

and (B-4)

$$\frac{Ac}{A} = \frac{p}{\beta L}$$

thus:

$$j = NTU\ N_{pr}^{2/3} \cdot \frac{1}{L} \cdot \frac{p}{\beta} \qquad \text{(B-27)}$$

It is apparent from (B-27)

$$j\ \alpha\ \frac{p}{\beta}$$

Heat Transfer Power and Flow Friction Power

An evaluation of the heat transfer power versus flow friction power is of interest in that it is a measure of relative performance.

Beginning with the definition of the Colburn-j factor:

$$j = N_{st} N_{pr}$$

$$N_{st} = \frac{N_{Nu}}{N_r N_{pr}} = \frac{hD_h}{k} \cdot \frac{k}{C_p \mu} \cdot \frac{1}{N_R}$$

therefore:

$$j = \frac{hD_h}{C p \mu} \cdot \frac{1}{N_R} \cdot N_{pr}^{2/3}$$

solving for h:

$$h = \frac{C p \mu}{N_{pr}^{2/3}} \cdot \frac{1}{D_h} \cdot N_R \, j \qquad \text{(B-28)}$$

If C_p , μ , and N_{pr} are evaluated at standard conditions of dry air at 500°F and one atmosphere [10]

$cp = 0.2477$ BTU/lb-F

$\mu = 0.0678$ lb/hr-ft

$\rho = 0.0413$ lb/ft^3

$N_{pr} = 0.671$

Equation (B-28) becomes:

$$h_{std} = 0.02195 \left(\frac{1}{4 r_h}\right) (N_R j) \qquad \frac{\text{BTU}}{\text{hr-ft}^2 - {}^\circ\text{F}} \qquad \text{(B-29)}$$

The flow friction power per unit area is derived as follows:

$$f = 2gc \, \rho m \frac{\Delta P}{G^2} \left(\frac{r_h}{L} \right) \qquad \text{rearranging}$$

$$\Delta P \; \frac{r_h}{L} = \frac{G^2 f}{2gc \; \rho m} \text{, since } G = \rho m V$$

$$E = \Delta P \frac{r_h}{L} \left(\frac{V}{550}\right) = f \left[\frac{1}{2gc} \left(\frac{1}{4 r_h}\right)^3 \frac{\mu^3}{\rho_m^2} \left(\frac{\rho m V D h}{\mu} \right)^3 \right]$$

therefore:

$$E = \frac{1}{2gc} \; \frac{\mu^3}{\rho_m^2} \left(\frac{1}{4 r_h}\right)^3 \; f \; N_R^3 \qquad \text{(B-30)}$$

When equation (B-30) is evaluated at standard conditions (μ and ρ_m values given above), the flow friction power per unit area at Standard conditions is:

$$E_{STD} = 1.11 \times 10^{-7} \quad \frac{1}{D_h^3} \quad f \left(\frac{N_R}{1000}\right)^3 \ \mathrm{HP/ft^2} \tag{B-31}$$

For comparison purposes the surface geometries were reduced to a common hydraulic diameter of $D_h = 2. \times 10^{-3}$ ft.

APPENDIX C

Description of Equipment

The equipment utilized to obtain the data from which the heat transfer and flow friction characteristics were determined was basically the same for both methods of testing. Only one change was required, and that was in the power equipment to produce the necessary temperature change corresponding to the method employed.

This appendix will be divided into two main subsections;

(1) Equipment common to the cyclic and single blow testing systems

(2) Power generating equipment utilized

1. Equipment common to the cyclic and single-blow testing systems

Fluid Source:

Air, the working fluid, was drawn through the test apparatus by a 30HP, multistage, Spencer Turbo-Compressor rated at 550cfm operating on a 220 volt a.c. power supply.

Flow Metering System:

Flow rates were measured by means of an ASME standard orifice section designed for convenient changing of orifice plates [7]. Thin plate concentric orifices with throat diameters from .775 to 2.31 inches were employed. The inside pipe diameter, d, was 3.08 inches. Pressure taps were located one pipe diameter upstream and one-half pipe diameter downstream from the orifice.

Fluid Heater System:

The air heater section consisted of 28 nichrome .0031" diameter wire heaters. Nichrome was selected because of its high resistivity, low thermal conductivity, and low specific heat.

The nichrome wire was wound on bakelite frames, two heaters to a frame. The wires were wound 1/32" apart, 50 and 52 wires respectively to each heater, and were formed into a rectangular mesh. The heaters on each frame were electrically connected in parallel and then connected through a toggle switch to voltage bus bars.

A schematic wiring diagram for one frame is shown below:

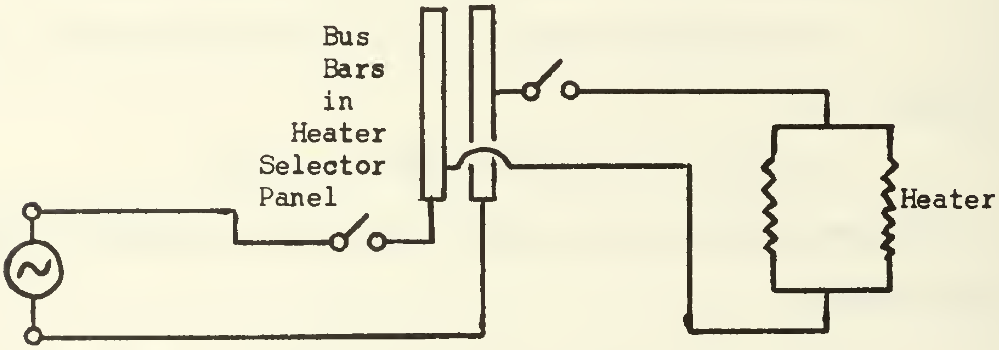

All heaters selected operate in parallel when power was applied. The number of heaters used was dependent on the testing method. For single blow testing the number of heaters used was determined by the number required to effect a 20°F rise for a given mass flow rate when a 220 volt source was applied, e.g., at $\dot{m}$ = 790. lbm/hr and V = 220 a.c., 22 heaters were required. For cyclic testing all 28 heaters were used while the input voltage was varied.

Matrix Holder and Test Section (Figure 4)

The matrix holder and test section were constructed from polyethylene plastic. The test section casing contained a removable frame on which a set of five thermocouples connected in series was mounted, T_2. It also contained two static pressure taps, one upstream and one downstream from the matrix holder. The components making up the casing and holder were machined to close tolerances, thereby minimizing air leakage, and insuring good alignment of the flow channel through the system. The flow channel was 3-3/16" by 3-3/16". Matrices with flow lengths up to 3" could be tested. Another removable thermocouple frame containing a set of five thermocouples connected in series, T_4 , was mounted in the exit plane of the matrix holder. The matrices were placed in the holder and held in place by insertion of styrofoam plastic on four sides of the matrix to insure a snug fit in the holder and proper position relative to the gas flow.

Pressure Measuring System

Pressure taps were located upstream and downstream from the matrix holder and on either side of the orifice. Each tap was connected to an appropriate manometer or draft gage via Imperial Company "poly-flow" tubing. The following instruments were utilized:

(1) E. Vernon Hill and Company Type "C" Micromanometer, 0-125"
(2) Ellison Draft Gage Company, 0-3.0" inclined gage
(3) Ellison Draft Gage Company, 10" manometer
(4) Ellison Draft Gage Company, 20" manometer
(5) Merriman Instrument Company, 50" manometer
(6) Merriman Instrument Company, 120" manometer

Any one of the above instruments or combination could be used to measure the differential pressures at the orifice or matrix. Cross checking of the various instruments assured reliable operation.

Temperature Measuring System: (Figure 1)

All temperatures were measured with thermocouples. There were four locations in the system where a temperature was monitored; prior to the flow straightner, before and after the matrix, and before the orifice.

A 30 gage copper-constantan thermocouple upstream from the orifice plate was referenced to an ice junction. The output was read from a Rubicon Company Portable Precision Potentimeter.

Four sets of 30 gage iron-constantan thermocouples were utilized at the remaining three positions. Each of the four sets was made up with five thermocouples connected in series. All 20 thermocouples were of similar construction and were fabricated from the same spools of iron and constantan wire. Thirty iron-constantan couples were made up and tested for temperature response (1) with the aid of a Leeds and Northrop Company, Type K-3 Universal Potentimeter. From the couples tested the 20 thermocouples that had the lease diviation from the average output were selected. The maximum deviation from the average output of the thermocouples selected was 018 ± .2 μv.

Two of the four sets of iron-constantan thermocouples were inserted into a 1/4" diameter aluminum tube which served as a radiation shield. The tube was mounted in a frame located at the exit of the contracting cone. All ten thermocouples in the two sets were individually wrapped with teflon tape to prevent shorting. Each set was designated as T_1. Another set, T_2, of five thermocouples connected in series was securely mounted in a frame in the test section located immediately upstream from the matrix. The remaining set of thermocouples was mounted in a frame located in the exit plane of the matrix holder. The latter set was designated T_3. The output of T_2 and T_3 were individually referenced to the outputs of the two T_1's located upstream at the entrance to the system. Therefore, the output of (T_1 vs T_2) represented the magnitude of the temperature rise of the heated air above ambient entering the matrix, and (T_1 vs T_3) sensed the temperature rise of the exiting gas from the matrix above ambient.

For the single blow tests a record of the output of (T_1 vs. T_3) as a function of time was made for each run. For the cyclic tests the outputs of (T_1 vs T_2) and (T_1 vs T_3) were recorded. The recording instrument was a Mosely Company, Model 7100B dual channel strip chart recorder. Sixteen fixed full span settings or any magnitude of voltage span from 1 millivolt to 100 volts were available for selection. Twelve fixed chart speeds in the range of 1 inch per hour to two inches per second were provided.

2. Power Generating Equipment Utilized.

For the single blow test runs the power to the heaters was supplied by a 240 volt a.c., 60 cycle source regulated by a General Radio Company Type W20HM "Variac" auto transformer, 0-240 volt, 8 amp load capacity.

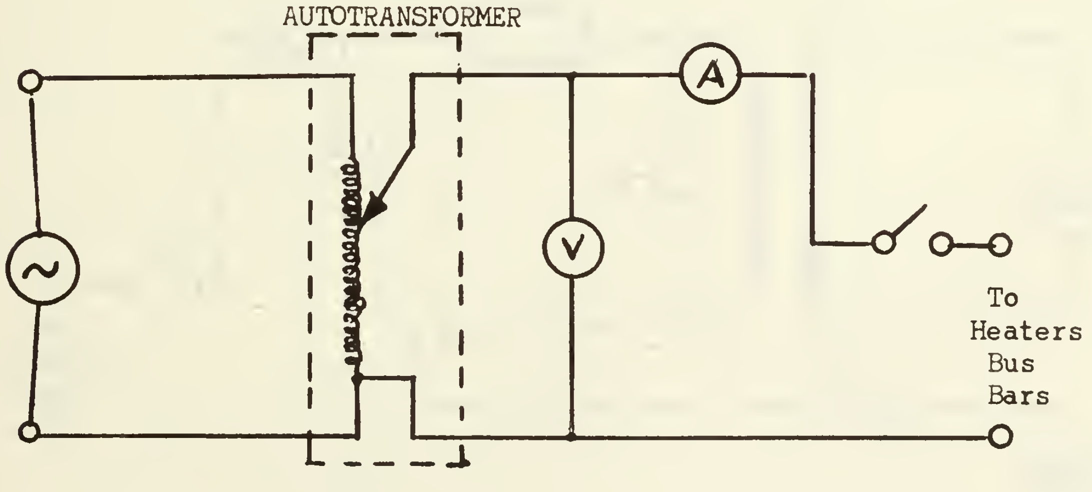

With the arrangement shown above schematically, the amount of voltage supplied to the resistive heaters could be simply regulated. The on-off knife switch provided a means by which the power could be quickly secured.

The cyclic technique required a means of creating a low frequency sinusoidal temperature wave. The frequency range was dictated by the core material and mass flow rate for each test run. This restriction is implied by the requirement of keeping the flow parameter, M < 0.1. At the maximum mass flow rate of 2000. lbm/hr used during testing the maximum frequency required was 2.1 cycles per second.

The system finally employed to fulfill the requirements of the cores reported consisted of a 1.5 KW, 3 phase, 1725 RPM, inductively wound G.E. amplidyne motor generator and a Hewlett Packard, Model 203A low frequency function generator. The schematic drawn below indicates the manner in which these components were used.

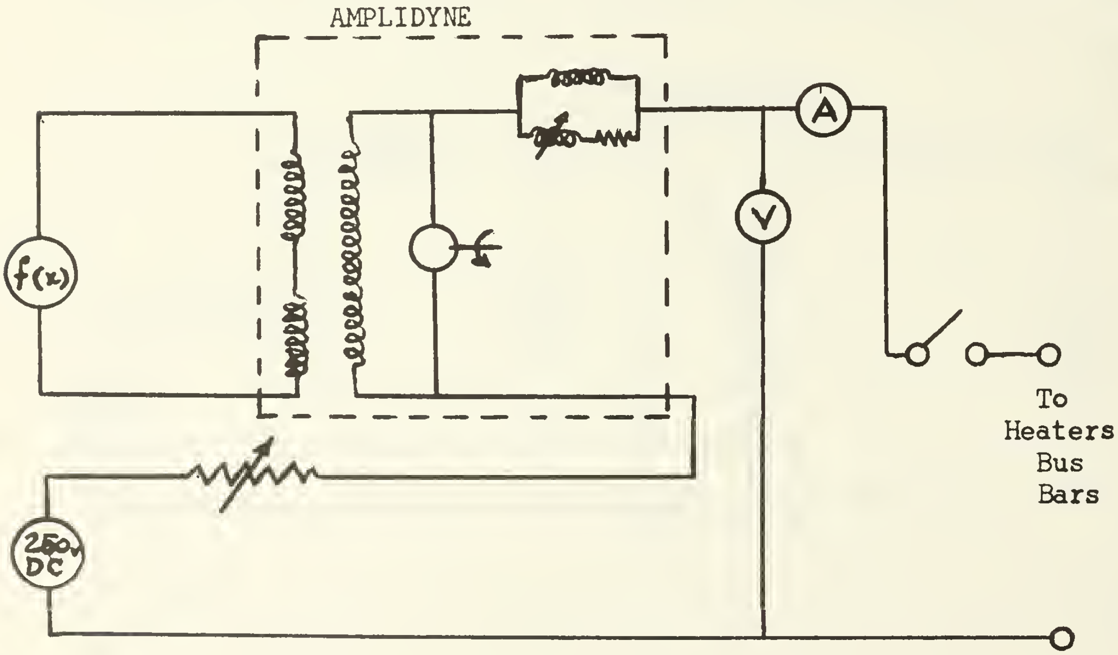

The function generator's voltage, amplitude, and frequency output controlled the field excitation of the amplidyne. The output level of the amplidyne was raised above electrical ground by an amount controlled by the setting of a high wattage resistance box connected in series with a 250 volt coarsely regulated d.c. generator. The magnitude of the d.c. voltage fixed the mean temperature, t_m, of the flowing gas.

The frequency response was relatively flat up to approximately 1.2 cps. Its peak to peak voltage output in this frequency range was 80 volts. As the system was driven faster by the function generator the peak to peak voltage amplitude decreased to about 30 volts at 2.5 cps.

APPENDIX D. PERFORATED NICKEL PROPERTIES

The perforated nickel plate fins of the Solar #2 matrix is an electro-deposited metallic sheet of integral structure manufactured by Perforated Products, Incorporated, and is designated by the manufacturer as 80/20T. The material is .0047 inches thick with 14% open area formed by slotted holes nominally .0023 inches by .034 inches, the centers of which are spaced .0125 inches in the flow direction and .050 inches transverse.

For a solid splitter plate or solid fin, the conduction parameter is defined as

$$\lambda = \frac{k_s A_s}{L\ C}$$

where A_s is the solid cross-sectional area for conduction which is equal to the product of plate width and thickness, and L is the conduction path length which is identical to the matrix flow length. The grouping of terms $\frac{L}{k_s A_s}$ represents the thermal conduction resistance, thus, the conduction parameter may be expressed as

$$\lambda = \frac{1}{R_{th} C} \qquad \text{where} \quad R_{th} = \frac{L}{k_s A_s}$$

Using this form, the conduction parameter for a perforated material will be represented by

$$\lambda_k = \frac{1}{(R_{th})_k C}$$

It is useful to define a relative conduction shape factor, S^*, such that

$$S^* = \frac{R_{th}}{(R_{th})_k} = \frac{\lambda_k}{\lambda}$$

Thus S^* is seen to be the ratio of the conduction parameter of a perforated material to the conduction parameter of the same material unperforated.

By analogy between conduction heat transfer and electric current, the ratio of electrical resistances to current flow of two specific geometrical shapes, is equal to the ratio of thermal conduction resistances to heat flow in the same direction. Thus

$$\frac{r}{r_k} = \frac{R_{th}}{(R_{th})_k}$$

Two dimensional models were constructed from electrically conducting paper (Teledeltos paper) representing repeatable sections of the perforated material and its unperforated counterpart. Figure 26 is a plan view of the perforated material, the shaded portion representing the repeatable section. Figure 27 below it shows the two shapes for which the resistances were compared. Measuring the resistances with an ohm-meter yielded the ratio of electrical resistances

$$\frac{r}{r_k} = \frac{R_{th}}{(R_{th})_k} = S^* = \frac{\lambda_k}{\lambda}$$

Finally, the conduction parameter for the perforated material is obtained

$$\lambda_k = S^*\lambda \qquad \text{where} \quad \lambda = \frac{k_s A_s}{L\ C}$$

UNCLASSIFIED
Security Classification

DOCUMENT CONTROL DATA - R&D

(Security classification of title, body of abstract and indexing annotation must be entered when the overall report is classified)

1. ORIGINATING ACTIVITY *(Corporate author)*
Naval Postgraduate School
Monterey, California 93940

2a. REPORT SECURITY CLASSIFICATION
Unclassified

2b. GROUP
X

3. REPORT TITLE
Heat Transfer and Flow Friction Characteristics of Several Plate-Fin Type Compact Heat Exchanger Surfaces

4. DESCRIPTIVE NOTES *(Type of report and inclusive dates)*
Task Progress, July 65 - June 67

5. AUTHOR(S) *(Last name, first name, initial)*
Pucci, P. F.
Ball, S. F., Jr.
Traister, R. E.

6. REPORT DATE
31 August 1967

7a. TOTAL NO. OF PAGES
61

7b. NO. OF REFS
12

8a. CONTRACT OR GRANT NO.

b. PROJECT NO.

c.

d.

9a. ORIGINATOR'S REPORT NUMBER(S)
NPS-59PC7081A

9b. OTHER REPORT NO(S) *(Any other numbers that may be assigned this report)*

10. AVAILABILITY/LIMITATION NOTICES
This document has been approved for public release and sale; its distribution is unlimited.

11. SUPPLEMENTARY NOTES

12. SPONSORING MILITARY ACTIVITY
Naval Ship Systems Command - Code 6146

13. ABSTRACT

Experimental results for the convective heat transfer and flow friction characteristics of plate-fin type heat transfer surfaces are presented for five surfaces. Four surfaces had a sinusoidal fin geometry. Two of these were fabricated of stainless steel, two of nickel. One of the nickel surfaces had perforated nickel fins. The fifth surface was fabricated of stainless steel and had a triangular fin geometry. The heat transfer data were obtained by the single-blow transient testing technique and by the cyclic testing technique. The two techniques compliment each other in extending the range of testing capability.

DD FORM 1 JAN 64 1473

UNCLASSIFIED
Security Classification

UNCLASSIFIED

Security Classification

14 KEY WORDS	LINK A		LINK B		LINK C	
	ROLE	WT	ROLE	WT	ROLE	W
Heat Exchangers						
Heat Transfer Surfaces						
Regenerators						
Recuperators						

DISTRIBUTION LIST

Commander
Naval Ship Systems Command
Washington, D.C. 20360
ATTN: Code 6146 (20 copies)

Commander
Naval Ship Systems Command
Washington, D.C. 20360
ATTN: Code 00G

Commander
Naval Ship Systems Command
Washington, D.C. 20360
ATTN: Code 034

Commanding Officer
Office of Naval Research
Branch Office
Box 39
Fleet Post Office
New York 09510

Commanding Officer
Office of Naval Research
Branch Office
219 South Dearborn St.
Chicago, Illinois 60604

Commanding Officer
Office of Naval Research
Branch Office
1076 Mission St.
San Francisco, Calif. 94103

Navy Ship Research & Development Center
Carderock, Maryland
ATTN: Library

Librarian
Special Devices Center
Port Washington, New York

Librarian
Navy Intelligence School
Naval Receiving Station
Washington 25, D.C.

Commander
Naval Ordnance Laboratory
White Oak, Silver Springs
Maryland 20910
ATTN: Librarian

Office of the Asst. Naval
Attache for Research
Naval Attache, American Embassy
Navy No. 100, Fleet P.O.
New York, New York

Naval Weapons Center
China Lake, California 93555
ATTN: Technical Library

Chief Scientist
Office of Naval Research
Branch Office
1030 East Green Street
Pasadena, California 91101

Commanding Officer and Director
Navy Electronics Lab. (Library)
San Diego, California 92152

Librarian
Naval Ordnance Systems Command
Washington, D.C. 20360

Director
Naval Research Laboratory
Washington, D.C. 20390
ATTN: Code 2027

Librarian
Technical Library, Code 245L
Building 39/3
Boston Naval Shipyard
Boston, Massachusetts 02129

Naval Applied Science Laboratory
Technical Library
Building 291, Code 9832
Naval Base
Brooklyn, New York 11251

Commander
Philadelphia Naval Shipyard
Philadelphia, Pennsylvania 19112
ATTN: Librarian, Code 249c

AFOSR
ATTN: SREM
Washington 25, D.C.

Aro, Incorporated
AEDC Library
Arnold Air Force Stn.
Tennessee
ATTN: Tech. Files

AiResearch Mfg. Company
9851-9951 Sepulveda Blvd.
Los Angeles, Calif. 90009
ATTN: Dr. P.J. Berenson

AiResearch Mfg. Company
9851-9951 Sepulveda Blvd.
Los Angeles, Calif. 90009
ATTN: F. E. Carroll

AiResearch Mfg. Company
402 South 36th Street
Phoenix Arizona
ATTN: Engrg. Library

The Air Preheater Co.
Wellsville, N.Y., 14895
ATTN: Engrg. Library

Allis-Chalmers Mfg. Co.
General Machinery Div.
Milwaukee 1, Wisconsin
ATTN: Mr. R. C. Allen, Dir.
of Mech. Engrg.

Alfred Amorosi
Atomic Power Dev. Assoc.
1911 First Street
Detroit 26, Michigan

Argonne National Lab.
Library Services Dept.
Report Sect.-Bldg. 14, Rm. 14
9700 South Cass Avenue
Argonne, Illinois, 60440

Office of the Asst. Chief of Staff,
G-4
Res. and Dev. Division
Dept. of the Army
Washington 25, D.C.

U. S. Army Ord. Missile Cmd.
Redstone Arsenal, Alabama
ATTN: AMSMI-RR, Bldg. 5429

David Aronson
Advanced Products Div.
Worthington Corp.
32 Green Street
Newark 2A, New Jersey

U. S. Atomic Energy Com.
Div. of Tech. Info. Ext.
P.O. Box 62
Oak Ridge, Tennessee 37831

Atomics International
P.O. Box 309
Canoga Park, Calif.
ATTN: Library

Avco Everett Res. Lab.
2385 Revere Beach Parkway
Everett 49, Mass.
ATTN: Tech. Library

The Babcock & Wilcox Co.
Res & Dev. Center
P.O. Box 835
Alliance, Ohio
ATTN: Library

Battelle Memorial Inst.
505 King Avenue
Columbus 1, Ohio
ATTN: Library

Brookhaven Nat. Lab.
Tech. Info Division
Upton, Long Island, N.Y.
Attn: Res. Library

NASA
Lewis Research Center
2100 Brookpark Road
Cleveland, Ohio 44135
ATTN: Library

NASA
Ames Research Center
Moffett Field, Calif.
ATTN: Library

NASA
Langley Research Center
Langley Station
Hampton, Virginia, 23365
ATTN: Library

Mr. A. J. Ede
Heat Division
Mech. Engrg. Res. Lab.
D.S.I.R., East Kilbride
near Glasgow, SCOTLAND

Office of the Administrator
NASA Headquarters
Washington D.C. 20546

University of New Mexico
Dept. of Mech. Engrg.
Albuquerque, New Mexico
ATTN: Engrg. Library

General Electric Co.
2151 So. 1st Street
Atomic Power Equip. Div.
San Jose, California
ATTN: Engrg. Library

General Motors Corp.
Harrison Radiator Dov.
Lockport, New York
ATTN: Engrg. Library

General Motors Corp.
Research Laboratories
12 Mile & Mound Roads
Warren, Michigan
ATTN: Engrg. Library

General Motors Crop.
Research Laboratories
12 Mile & Mound Roads
Warren, Michigan
ATTN: Mr. J. R. Mondt
Engrg. Dev. Dept.

Gulf Res. & Dev. Co.
P.O. Drawer 2038
Pittsburgh, Pa. 15230
ATTN: Engrg. Library

International Harvester Co.
Engineering Research Dept.
5225 S. Western Blvd.
Chicago 9, Illinois
ATTN: Engrg. Library

Mr. Richard Herold, Pres.
Sulzer Bros., Ltd.
19 Rector Street
New York, N.Y. 10006

Mr. Edward Hines, Director
Engineering Research Dept.
The Detroit Edison Co.
2000 Second Avenue
Detroit 26, Michigan

Prof. E. D. Howe, Director
Sea Water Conversion Lab.
University of California
1310 South 46th Street
Richmond, Calif.

Illinois Institute of Tech.
Dept. of Mech. Engrg.
Technology Center
Chicago 16, Illinois
ATTN: Heat Transfer Lab.

University of Illinois
Mechanical Engrg. Dept.
Urbana, Illinois
ATTN: Engrg. Library

M. W. Kellogg Co.
711 Third Avenue
New York 17, N.Y.
ATTN: Engrg. Library

Oregon State College
Corvallis, Oregon
ATTN: Engrg. Library

Mr. E. J. LeFevre
Dept. of Mech. Engrg.
Queen Mary College
LONDON E.1, ENGLAND

Brown Boveri Corp.
19 Rector Street
New York 6, N.Y. 10006
ATTN: E. H. Stauffer
Staff Assistant

University of California
College of Engrg.
Berkeley 4, California
ATTN: Prof. A. Oppenheim

California Inst. of Technology
1201 E. California St.
Pasadena 4, California
ATTN: Engrg. Library

University of California
College of Engrg.
Berkeley 4, California
ATTN: Prof. R. A. Seban, M.E.

Calif. Research Crop.
576 Standard Avenue
Richmond, California
ATTN: Engrg. Library

Case Inst. of Technology
University Circle
Cleveland 6, Ohio
ATTN: Engrg. Library

Caterpillar Tractor Co.
Peoria, Illinois, 61611
ATTN: Mrs. M. M. Landuyt
Res. Lib.

The Catholic University of America
Dept. of Mech. Engrg.
Washington 17, D.C.
ATTN: Prof. C. P. Howard

Chance-Vought Aircraft
Dallas, Texas
ATTN: Library

Dr. D. L. Cochran
M & B Associates
P.O. 196
San Ramon, Calif.

Columbia University
Heat Trans. Res. Fac.
632 W. 125th St.
New York 27, New York

Cooper Bessemer Corp.
Mt. Vernon, Ohio
ATTN: R. L. Boyer
V. Pres. & Chief Engnr.

Dynatech Corp.
17 Tudor Street
Cambridge, Mass.

Eitel-McCullough, Inc.
301 Industrial Way
San Carlos, California
ATTN: Tech. Library

NPFO, U. S. Army Engineer
Reactors Group
Ft. Belvoir, Va. 22060
ATTN: Supervisor, Staff Engrg.
Dept./NPFO Bldg. T-2384

The Franklin Institute
Labs. for Res & Dev.
Philadelphia 3, Pa.
ATTN: Engrg. Library

The M. W. Kellog Co.
711 Third Avenue
New York 17, N.Y.
ATTN: Engrg. Library

General Electric Co.
Main Library
Schenectady 5, New York 12305
ATTN: Miss A. Ruane

General Electric Co.
1000 Western Ave.
West Lynn 3, Mass.
ATTN: Engrg. Library

Prof. R. W. Stuart Mitchell
Laboratorium voor Verbrandingsmotoren en Gasturbines der
Technische Hogeschool
Mekelweg 2
Delft, HOLLAND

Logan Lewis Library
Carrier Research & Dev.
Carrier Parkway
Syracuse, New York 13201

Lockheed Aircraft Co.
Technical Library
Burbank, California
ATTN: B. L. Messinger,
Engr. N. 7225

Mr. R. E. Lundberg
Vidya Inc.
1450 Page Mill Road
Palo Alto, Calif.

Mass. Inst. of Technology
Cambridge, Mass. 02139
ATTN: Prof. W. H. McAdams
Chem. Engrg.

Mass. Inst. of Technology
Cambridge, Mass. 02139
ATTN: Prof. W. M. Rohsenow
Mech. Engrg. Rm. 1-212

Mass. Inst. of Technology
Cambridge, Mass. 02139
ATTN: Prof. E. S. Taylor
Gas Turbine Lab.

McGraw-Hill Publishing Co.
330 West 42nd Street
New York 36, N.Y.
ATTN: L. N. Rowley, Editor &
Publisher, POWER

New York University
Dept. of Mech. Engrg.
University Heights
New York 53, N.Y.
ATTN: Prof. Fred Landis

North American Aviation, Inc.
International Airport
Los Angeles 9, Calif.
ATTN: Engrg. Library

Oak Ridge National Lab.
Y-12 Technical Library
P.O. Box Y
Oak Ridge, Tenn. 37831

Minneapolis-Honeywell
600 North Second
Hopkins, Minnesota
ATTN: Engrg. Library

Librarian
Republic Aviation Corp.
Farmingdale, Long Island
New York

K. C. Rosenbert, Supervisor
Technical Document Center
Hughes Aircraft Company
Florence & Teale Sts.
Culver City, Calif.
ATTN: MS E-110

Prof. R. K. Pefley
University of Santa Clara
Santa Clara, Calif.

University of Florida
Gainesville, Florida
ATTN: Engrg. Library

Librarian
Shell Development Co.
Emeryville, Calif.

Lear Siegler, Inc.
Engineering Library
P.O. Box 6719
Cleveland, 1, Ohio

Mr. P. A. Pitt
Vice Pres. Engrg/Rex.
Solar Aircraft Co.
2200 Pacific Highway
San Diego 12, Calif.

Librarian
Solar
2200 Pacific Highway
San Diego, Calif. 92112

Space Tech. Lab., Inc.
Space Tech. Center
One Space Park
Redondo Beach, Calif.
ATTN: Engrg. Library

Air Preheater Co.
Wellsville, New York
ATTN: T. Evans

Air Preheater Co.
Wellsville, New York
ATTN: G. Theoclotis

Hamilton Standard
Div. of UAC
Windsor Locks, Conn.
ATTN: Mr. A. Watnabe

Mr. H. T. Pledge
Keeper of the Library
The Science Library
Science Museum
South Kensington
London, S.W. 7, ENGLAND

Central Order Records
Technical Info. Library
Bell Telephone Labs
463 West Street
New York 17, New York

Librarian
University of Oklahoma
Norman, Oklahoma

Librarian
University of Pennsylvania
Philadelphia, Pennsylvania

Librarian
NASA
1512 H Street
Washington, D.C.

Mr. V. J. Klein
Regenerator Project Engr.
The Boeing Co.
Turbine Div.
P.O. Box 3955
Seattle, Washington 98124

Documents Department
General Library
University of California
Berkeley, California 94720

Lockheed-California Company
Central Library
Dept. 77-14, Bldg. 170, Plt. B-1
Burbank, California 91503

Serials Dept., Library
University of California, San Diego
La Jolla, California 92038

Aircraft Division
Douglas Aircraft Company, Inc.
3855 Lakewood Boulevard
Long Beach, California 90801
ATTN: Technical Library

Librarian
Government Publications Room
University of California
Los Angeles 24, California

General Dynamics/Convair
P.O. Box 1950
San Diego, California 92112
ATTN: Engineering Library
Mail Zone 6-157

Ryan Aeronautical Company
ATTN: Technical Information
Services
Lindbergh Field
San Diego, California 92112

General Electric Company
Technical Information Center
P.O. Drawer QQ
Santa Barbara, California 93102

Library
Boulder Laboratories
National Bureau of Standards
Boulder, Colorado

Government Documents Division
University of Colorado Libraries
Boulder, Colorado 80304

The Library
United Aircraft Corporation
400 Main Street
East Hartford, Connecticut 06108

Stanford Research Institute
Menlo Park, California
ATTN: S. H. Clark, Industrial
Econ. Div.

Prof. A. L. London
Stanford University
Dept. of Mech. Engrg.
Stanford, California

Stanford University
Stanford, Calif.
ATTN: Engineering Library

Stewart Warner Corp.
1514 Drover Street
Indianapolis 7, Indiana
ATTN: Library

Syracuse University
Syracuse 10, New York
ATTN: Engrg. Library

Allison Division
General Motors Co.
Indianapolis, Indiana
ATTN: Engrg. Library

Tufts University
Mech. Engrg. Dept.
Medford, Mass. 02155
ATTN: Engrg. Library

Vidya, Div. Itek Corp.
1450 Page Mill Road
Palo Alto, Calif.
ATTN: Librarian

Virginia Polytechnic Inst.
Blacksburg, Virginia
ATTN: Carol Newman, Library

Vitro Libraries
200 Pleasant Valley Way
West Orange, New Jersey
ATTN: Library

Engineering Library
213 Guggenheim
University of Washington
Seattle, Washington 98105

Westinghouse Electric Co.
Lester Branch P.O.
Philadelphia 13, Pa.
ATTN: Engrg. Library

Westinghouse Electric Co.
Bettis Atomic Power Lab.
P.O. Box 1468
Pittsburg 30, Pa.
ATTN: Technical Library

Westinghouse Electric Co.
306 4th Avenue
Pittsburg, Pa.
ATTN: Library

U. S. Military Academy
West Point, New York
ATTN: Library

University of Wisconsin
1513 University Ave.
Madison 5, Wisconsin
ATTN: Engineering Library

Mr. Stanley Wong
1128 West 126th Street
Los Angeles, Calif. 90044

Inst. of Tech. Library
MCLI-LIB, Bldg. 125, Area B
Wright-Patterson AFB
Ohio

ARL (AFRO)
Wright-Patterson AFB
Ohio
ATTN: RRLA Library

AMC
Wright-Patterson AFB
Ohio
ATTN: Library

Mrs. L. B. Phillips, Supt
Tech. Info. Section
Scientific Lab.
Ford Motor Co.
Dearborn, Mich.

Mr. Wm. A. Compton
Asst Director of Research
Solar
2200 Pacific Highway
San Diego, Calif. 92112

Documents Division
Yale University Library
New Haven, Connecticut

George Washington University Library
2023 G Street, N. W.
Washington, D.C. 20006

National Bureau of Standards Library
Room 301, Northwest Building
Washington, D.C. 20234

University of Chicago Library
Serial Records Department
Chicago, Illinois 60637

Documents Department
Northwestern University Library
Evanston, Illinois

The Technological Institute, Library
Northwestern University
Evanston, Illinois

Librarian
Purdue University
Lafayette, Indiana

John Hopkins University Library
Baltimore
Maryland 21218

Martin Company
Science-Technology Library
Mail 398
Baltimore, Maryland 21203

Scientific and Technical Information
Facility
ATTN: NASA Representative
P.O. Box 5700
Bethesda, Maryland 20014

Documents office
University of Maryland Library
College Park, Maryland 20742

The Johns Hopkins University
Applied Physics Laboratory
Silver Spring, Maryland
ATTN: Document Librarian

Massachusetts Institute of Technology
Serials and Documents
Hayden Library
Cambridge 39, Massachusetts

Technical Report Collection
303A, Pierce Hall
Harvard University
Cambridge 38, Massachusetts
ATTN: Mr. John A. Harrison,
Librarian

Alumni Memorial Library
Lowell Technological Institute
Lowell, Massachusetts

Librarian
University of Michigan
Ann Arbor, Michigan

Gifts and Exchange Division
Walter Library
University of Minnesota
Minneapolis, Minnesota 55455

Reference Department
John M. Olin Library
Washington University
6600 Millbrook Boulevard
St. Louis, Missouri 63130

Librarian
Forrestal Research Center
Princeton University
Princeton, New Jersey 08540

Engineering Library
Plant 25
Grumman Aircraft Engineering Corp.
Bethpage, L. I., New York 11714

Librarian
Fordham University
Bronx 58, New York

Librarian
Cornell Aeronautical Laboratory
4455 Genesee Street
Buffalo 21, New York

Central Serial Record Dept.
Cornell University Library
Ithaca, New York 14850

Columbia University Libraries
Documents Acquisitions
535 W. 114 Street
New York, New York 10027

Engineering Societies Library
345 East 47th Street
New York, New York 10017

Library-Serials Department
Rensselaer Polytechnic Institute
Troy, New York 12181

Librarian
Documents Division
Duke University
Durham, North Carolina

Ohio State University Libraries
Serial Division
1858 Neil Avenue
Columbus 10, Ohio

Steam Engineering Library
Westinghouse Electric Corporation
Lester Branch Post Office
Philadelphia, Pennsylvania 19113

Hunt Library
Carnegie Institute of Technology
Pittsburgh 13, Pennsylvania

Documents Division
Brown University Library
Providence, Rhode Island 02912

Documents Division
The Library
Texas A & M University
College Station, Texas 77843

Librarian
LTV Vought Aeronautics Division
P.O. Box 5907
Dallas, Texas 75222

Defense Documentation Center (DDC)
Cameron Station
Alexandria, Virginia 22314
ATTN: LRS (20 copies)

Naval Postgraduate School
Code 02
Code 023
Code 0212 (2 copies)
Code 59Pc (20 copies)

DUDLEY KNOX LIBRARY
3 2768 00396463 6